Thesis for the degree of Doctor of Philosophy

Microwave Gas and Multipactor Breakdown in Inhomogeneous Fields

Joel Rasch

Department of Earth and Space Sciences
Chalmers University of Technology
Göteborg, Sweden, 2012

Microwave Gas and Multipactor Breakdown in Inhomogeneous Fields
Joel Rasch

ISBN 978-91-7385-757-4
Doktorsavhandlingar vid Chalmers tekniska högskola
Ny serie nr 3438
ISSN 0346-718X

Department of Earth and Space Sciences
Non-Linear Electrodynamics
Chalmers University of Technology
SE–412 96 Göteborg
Sweden
Telephone +46–(0)31–772 10 00

Printed in Sweden by
Reproservice
Chalmers Tekniska Högskola
Göteborg, Sweden, 2012

Microwave Gas and Multipactor Breakdown in Inhomogeneous Fields

Joel Rasch
Department of Earth and Space Sciences
Chalmers University of Technology

Abstract

Microwave gas and multipactor breakdown remains to be one of the limiting factors for the maximum power in microwave devices. Above a certain electric field strength, the so-called breakdown threshold, free electrons can multiply by making ionizing impacts with neutral gas molecules, or causing secondary emission upon impact with system surfaces. The free electron number will rise exponentially, and a number of problems may arise, ranging from noise and changes in the device impedance, to the melting of metal parts and possible destruction of the system.

In this thesis we focus our attention at certain aspects of microwave breakdown in satellites and space related systems. This entails air breakdown during testing on ground and ascent, as well as multipactor breakdown in the vacuum of orbit. Our approach to the breakdown problem is a purely theoretical one. Starting from well known physical laws and empirical approximations we apply them to novel systems in an effort to determine the breakdown characteristics.

For the case of gas breakdown, our main concern in this thesis has been on analyzing the effect of there being small regions of field enhancement or gas heating inside the microwave system. We try to answer the questions: under what circumstances can small regions of breakdown plasma expand and cause full scale breakdown, and what might be the effect of having local heating of the gas?

In the case of multipactor, all our research have sprung from the analysis of a complicated quadri-filar helix antenna. The open geometry, curved surfaces, and large wire separation has lead us to explore an approximate model for the electron dynamics: where the trajectories are dictated by the geometry of the emitting surface, and the action of the ponderomotive force; and the electron impacts can be treated using statistical methods.

Keywords: Microwave breakdown, multipactor, corona, inhomogeneous fields

Publications

[A] J. Rasch, D. Anderson, M. Lisak, V. E. Semenov, and J. Puech, "Microwave Corona Breakdown in a Gas-Filled Rectangular Resonator Cavity", J. Phys. D: Appl. Phys. **42**, 055210 (2009).

[B] J. Rasch, D. Anderson, M. Lisak, V. E. Semenov, and J. Puech, "Gas Breakdown in Inhomogeneous Microwave Electric Fields ", J. Phys. D: Appl. Phys., **42**, 205203 (2009).

[C] J. Rasch, D. Anderson, J. Johansson, M. Lisak, J. Puech, E. Rakova, and V. E. Semenov, "Microwave Multipactor Breakdown Between Two Cylinders", IEEE Trans. Plasma Sci., **38**, 8, 1997 (2010).

[D] J. Rasch, V. E. Semenov, D. Anderson, M. Lisak, and J. Puech, "On the Microwave Breakdown Stability of a Spherical Hot Spot in Air", J. Phys. D: Appl. Phys., **43**, 325204 (2010).

[E] J. Rasch, V. E. Semenov, E. Rakova, D. Anderson, J. F. Johansson, M. Lisak, and J. Puech, "Simulations of Multipactor Breakdown Between Two Cylinders", IEEE Trans. Plasma Sci., **39**, 9, 1786 (2011).

[F] J. Rasch and J. F. Johansson, "Non-Resonant Multipactor - A Statistical Model", submitted to Phys. Plasmas (2012).

[G] J. Rasch, V. E. Semenov, and J. Puech, "Microwave Corona Breakdown around a Metal Ball in Air", submitted to J. Phys. D: Appl. Phys. (2012).

Other contributions (not included in the thesis)

[1] J. Rasch, D. Anderson, M. Lisak, V. E. Semenov, and J. Puech, "Microwave Corona Breakdown in Strongly Inhomogeneous Fields", 36th EPS Conference on Plasma Phys., Sofia, 2009 ECA, Vol. 33E, P-2.121 (2009).

[2] J. Rasch, D. Anderson, M. Lisak, V. E. Semenov, and J. Puech, "Microwave Corona Breakdown in RF Devices", PIERS Online, Vol. 5, No. 7, 613-616 (2009).

[3] D. Anderson, M. Desaix, M. Lisak, and J. Rasch "A Galerkin Approach to Approximate Solutions of some Nonlinear Oscillator Equations", Am. J. Phys., **78**, 9, 920 (2010).

[4] J. Rasch, D. Anderson, M. Lisak, V. E. Semenov, and J. Puech, "Thermal Stability of a Plasma in a Homogeneous Microwave Field in Air", 37th EPS Conference on Plasma Phys., Dublin, P1.316 (2010).

[5] J. Rasch, D. Anderson, J. Johansson, M. Lisak, J. Puech, E. Rakova, and V. E. Semenov, "Multipactor Breakdown in Open Two-Wire Transmission Lines", 32nd ESA Antenna Workshop on Antennas for Space Applications, ESTEC, Noordwijk, The Netherlands (2010).

[6] J. Rasch, V. E. Semenov, D. Anderson, M. Lisak, and J. Puech, "On the Thermal Balance of a Small Spherical Microwave Breakdown Region in Atmospheric Air", Strong Microwaves and Terahertz Waves: Sources and Applications, Nizhny Novgorod - St. Petersburg, Russia (2011).

[7] V. E. Semenov, E. Rakova, J. Rasch, D. Anderson, J. F. Johansson, J. Puech, and M. Lisak, "Study of the Multipactor Avalanche in Two-Wire Transmission Lines", Strong Microwaves and Terahertz Waves: Sources and Applications, Nizhny Novgorod - St. Petersburg, Russia (2011).

[8] J. Puech, D. Anderson, M. Lisak, E. I. Rakova, J. Rasch, V. E. Semenov, and I. A. Shereshevskii, "Summary of Research Activities on Microwave Discharge Phenomena Involving Chalmers (Sweden), Institute of Applied Physics (Russia), and CNES (France)", Mulcopim, Valencia (2011).

[9] J. Rasch, V. E. Semenov, D. Anderson, M. Lisak, and J. Puech, "The Nonlinear Evolution of a Small Spherical Microwave Breakdown Plasma in Air", Mulcopim, Valencia (2011).

[10] J. Rasch, V. E. Semenov, D. Anderson, M. Lisak, and J. Puech, "Microwave Corona Breakdown Around Helix Antennas in Air", Mulcopim, Valencia (2011).

[11] J. Rasch, V. E. Semenov, E. Rakova, D. Anderson, J. F. Johansson, M. Lisak, and J. Puech, "Microwave Multipactor Breakdown in Helix Antennas, Theory and Simulations", Mulcopim, Valencia (2011).

[12] J. F. Johansson, and J. Rasch, "Non-Resonant Probabilistic Multipactor Calculations", Mulcopim, Valencia (2011).

[13] V. E. Semenov, N. A. Zharova, N. I. Zaitsev, A. K. Gvozdev, A. A. Sorokin, M. Lisak, J. Rasch, and J. Puech, "Reduction of the Multipactor Threshold Due to Electron Cyclotron Resonance", accepted for publication in IEEE Trans. Plasma Phys. (2012).

Bringing a normal research problem to a conclusion is achieving the anticipated in a new way, and it requires the solution of all sorts of complex instrumental, conceptual, and mathematical puzzles. The man who succeeds proves himself an expert puzzle-solver, and the challenge of the puzzle is an important part of what usually drives him on.

Thomas S. Kuhn, The Structure of Scientific Revolutions

Contents

Acknowledgements

I would like to express my gratitude to my supervisors, past and present: Professors Mietek Lisak, Dan Anderson, and Vladimir E. Semenov. These people have provided me with a job I like, stimulating and challenging tasks, moral support, and the collective experience of roughly 100 years of theoretical work in breakdown physics and related areas. Next I would like to thank my coworkers, mainly for the company and good times, but also for the various work-related discussions during the years. My family and friends deserve a thank you for being there, supportive and kind, acting as a tether to the real world, from which I have a tendency to sometimes drift. Lastly, I would like to thank our partners and sponsors: the French space agency, CNES; the Swedish National Space Research Program (NRFP); RUAG Space AB; and the Institute of Applied Physics (IAP), for financial support, scientific cooperation, and supplying us with a source of interesting physical problems. In particular I would like to thank Jerome Puech at CNES, Elena Rakova at IAP, and Joakim F. Johansson at RUAG.

List of symbols

Below is a list of the most important symbols used in the text.

α_i	Townsend's first ionization coefficient
α_r	Recombination coefficient
γ	Field intensification factor
δ	Skin depth
δ_m	Average fraction of energy loss in electron-neutral collision
ϵ	Dielectric constant
ϵ_0	Vacuum permittivity
ϵ_r	Relative permittivity
Λ	Diffusion length
μ	Mobility
μ_0	Vacuum permeability
ν_a	Attachment frequency
ν_c	Collision frequency
ν_i	Ionization frequency
ν_m	Effective frequency for momentum transfer
$\nu_{\text{net}} \equiv \nu_i - \nu_a$	Net ionization frequency
ρ	Density
σ	Electric conductivity
ω	Field radian frequency
a	Radius of sphere, typical size of protruding metal object
$\bar{B}, \quad \bar{\mathcal{B}}$	Real and complex magnetic field vectors
d	Parallel plates gap width
D	Diffusion coefficient
e	Electron charge
$\bar{E}, \ \bar{\mathcal{E}}$	Real and complex electric field vectors
$\bar{E}_0$	External electric field vector
E_{b}	Breakdown field
$\bar{E}_{\text{e}}$	Effective electric field

$\bar{F}$	Force vector
h	Length of field enhancement
k_{B}	The Boltzmann constant
l	Mean free path
L	Typical system dimension
L_a	Attachment length
m	Electron mass
M	Mass of neutral gas particle
n	Electron density
n_0	Ambient electron density
n_{c}	Critical electron density
N	Gas density
N_0	Gas density at atmospheric pressure and room temperature
p	Effective pressure
p_0	Atmospheric pressure, 760 Torr
$\bar{r}$	Position vector
S	Energy flux
t_e	Emission time
T	Temperature
T_0	Room temperature, 293 K
$\bar{u}$	Average velocity
$\bar{v}$	Velocity vector
$\bar{v}_d$	Drift velocity vector
$\bar{v}_{\mathrm{e}}$	Emission velocity vector
W	Energy

Chapter 1

Introduction

In the context of high power microwave equipment, microwave breakdown remains one of the limiting factors for the maximum allowable power and electric field strength. The appearance of a microwave discharge in the system can be very harmful, with effects ranging from noise and the creation of harmonics to the melting of vulnerable parts, destruction of dielectric windows, and the complete destruction of the system. The fundamental mechanism of breakdown in gas and vacuum is the avalanche multiplication of free electrons, either from electron impact ionization of electrically neutral gas molecules or secondary emission from surfaces due to electron impact. In order to avoid breakdown, formulate practical guidelines, and raise the allowable threshold power for breakdown, it is necessary to have a good understanding of the electron dynamics in both gases and vacuum. The purpose of this thesis is to give this basic understanding, which is required to understand the content of the included research articles, and to motivate the need for research into the topics of these articles. To provide this information in a coherent way, the thesis starts with a short historical review of gas discharge physics leading up to modern times. A glance at the history of the subject is not only entertaining, but it also gives an explanation to the nomenclature of the field, which can otherwise seem rather arcane.

The next section deals with the approximate results one finds when considering average electron motion. Although this approach is only moderately accurate for a limited number of results, it provides an intuitive feeling for what governs the dynamics of electron motion and avalanches. Using this simplified theory, we speculate about the behaviour of breakdown properties, and define two very important quantities: the effective electric field, and the effective pressure. After this section we dive deeper into how to

actually calculate the electrical breakdown threshold by using results from kinetic theory, together with empirical data for the ionization, attachment, and diffusion rates. The results in this section are applied to two simple scenarios: a parallel plate system with a homogeneous electric field, and a parallel plate system with a small field inhomogeneity. The calculations illustrate how to use the diffusion theory, how to present the results and what the main characteristics of the breakdown curves are. These results replicate the basic features found in papers A and B.

The section which concludes the discussion on gas breakdown provides an introduction to the main nonlinear effects and the effects of local gas heating and field intensifications. This discussion serves as an introduction to papers D and G.

The remaining part of the thesis deals with microwave breakdown in vacuum, so called multipactor. The basic physics is reviewed, and an overview of the classical resonance theory is given along with a discussion of why it fails for systems with long electron transit times. The nonresonant theory which is the subject of paper F is then introduced, and speculations on how to use it for systems more complicated than parallel plates are presented. Finally, it is described how to approximate electron trajectories in systems with long gap transit times using the concepts of geometrical spreading and the ponderomotive force, which were applied succesfully in papers C and E.

Chapter 2

Breakdown physics

The history of microwave breakdown has deep roots. It is impossible to separate the present subject from the historical and linguistic heritage of much earlier research. In the case of gas breakdown, the very first observations seem to have been made in ancient Greece, where amber was used in experiments with static electricity and miniature spark discharges. The greek word for amber - elektron - has stuck with us since these times, but systematic experiments were first conducted in the 17th and 18th centuries. The stories of these early researches into the field, and the theoretizing about the nature of electrical phenomena make for fascinating reading.

With the development of large batteries, it was possible to sustain the discharges for longer times, and in the beginning of the 19th century, the arc discharge was discovered almost simultaneously by Vasilii Petrov in St. Petersburg, and Humphry Davy at the Royal Institution in London [1]. The arc manifests itself as a bright conducting channel going between two electrodes. The name is derived from the way the channel tends to bend upwards in the middle, thus creating an arc-like shape. It seems likely that the roots of the term breakdown can be found at these times, for the conductivity of air at low electric field strengths is very small, and the rise in current with voltage is slow, until a certain voltage is reached, when suddenly the current rises dramatically, and the insulatory properties of the air seems to break down. The fact that the electrical conductivity of the air between electrodes changes so suddenly at a certain voltage led researchers to speculate about mechanical fractures in the very air surrounding the electrodes. Around the end of the 19th century there were a lot of different suggestions about the nature of this phenomena, but it was first with the work of J. J. Thompson and Townsend that the correct idea was formed.

Townsend suggested that the motion of electrons in the gas could explain the bulk of the observed phenomena [2]. In particular, the ionization of neutral gas molecules by energetic electrons was stated to be the cause of the sudden change of conductivity at a certain voltage. It was realised that at a certain field strength, electrons where able to gain enough energy to ionize the neutrals, and that this would lead to an exponential increase in the number of free electrons in very short intervals of time and space. Townsend also suggested that impact ionization due to positive ions might play an important role in the breakdown mechanism, but in this case he was quite wrong. The ions are far to heavy in comparison to the electrons to be of any importance when it comes to the ionization mechanism. The full incorporation of all the experimental results into a coherent theory could be accomplished first after the atom had been investigated. This stage was reached sometime around the 50's and the state of the art at that time along with a summary of the previous errors is nicely summarized in a large volume by Loeb [3].

The immediate breakdown mechanism under DC conditions is relatively easy to understand. It is caused by an avalanche multiplication of electrons moving towards the anode. The subsequent stages can be quite different. If the electrodes are made of a heat resistant metal, and the exterior circuit is able to maintain high currents, one will have an electric arc going between the electrodes. The arc is a column of high temperature air in the plasma state, electrons are liberated from the cathode by thermionic field emission, and impacts of ions, thus creating a closed current loop. By modifying the electrodes, quite different physical phenomena will become important. Sheath formation near the electrodes can be very important, and by using different gases instead of air, one will change the properties of the arc. By decreasing the pressure, the temperature of the arc will go down, and the discharge will become more diffuse, resulting in what is called a glow discharge. These are of a very large practical importance, for it is what is used in fluorescent lights. Where a glow discharge in mercury vapour creates UV light which interacts with the fluorescent inner coating of the tube to produce a glow that is comfortable to humans.

By changing the shapes of the electrodes, one will encounter new phenomena. If one of the electrodes is removed, the discharge will project outward from the single electrode into the surrounding air. Depending on the conditions, the discharge will appear as separated channels projecting outward from the electrode, or as a more diffuse halo surrounding it. Due to the appearance, and its tendency to appear at sharp edges and points, it has been coined the corona discharge from the latin word for crown. This

type of discharge is used frequently for a great multitude of applications, for example: the ozone that is generated is used to sanitize water, and the electrical properties are used in photocopiers. But it is also responsible for many unwanted effects. In particular, the loss of electrical energy around high voltage transmission cables, and the disturbances and corrosion which is created by corona discharges inside high power electrical devices.

By using a high frequency (instead of a DC) source to ignite a discharge in the gap between two electrodes, the ions and electrons will be oscillating back and forth in the gap, and given a sufficiently high frequency, only a very small number of charged particles will reach the electrodes and be absorbed. This basically removes the influence of the surrounding structures on the discharge mechanism itself, and any conducting surface will merely act as a sink for electrons reaching it by the process of diffusion. In this sense, microwave [1] discharges are much simpler to analyze than the range of physical processes that might be of importance for low frequency and DC conditions. It was with the invention of the magnetron that unwanted microwave discharges became a big problem. It was the limiting factor for the power output of radar systems during the Second World War, and consequently, a large amount of research was spent on developing reliable methods for predicting the power at which the air would suffer breakdown in different systems of practical interest. The formation of a discharge in a microwave system is very dangerous. At high pressures the gas will become very hot, and direct melting of conducting elements might be the result, whereas at lower pressures the deleterious effect will mainly be due to the electromagnetic disturbances caused by the conducting gas.

As soon as the war was over, the United States and the Soviet Union began research on the V2 rockets captured from Nazi Germany. It quickly became obvious that microwave breakdown around antennas mounted on high altitude rockets was a major problem. But due to the military nature of this research, the material that was openly published in the US is fragmentary, and in the Soviet virtually nonexistant. Since the phenomena was new at this time, and research was performed in separate entities using as a starting point the well established field of DC discharges, several names for the microwave breakdown phenomena were used. The two most common being microwave voltage breakdown, and microwave corona breakdown. The first designation is rarely used nowadays, but the latter has unfortunately

[1] The microwave range is often defined as the frequency range between 1 and 100 GHz. It is used for a great number of applications, e.g. microwave ovens, wireless internet, satellite communications, mobile phone networks, radar etc.

become prevalent in the space community. The fact that the term corona is used both for a DC and microwave phenomena often causes confusion, because the mechanisms are rather different, but it is simply due to the similar visual appearance of these discharges and the historical heritage of the field.

The most critical question to answer when dealing with high frequency breakdown is: at what electrical field strength or power level does breakdown occur? In other words, what is the breakdown threshold? Many different approaches for obtaining the answer can be found in open publications, and an excellent summary of the early phase (30's to 50's) can be found in a rather recent thesis by Price [4].

In 1948 Herlin and Brown at MIT published a paper in the Physical Review [5] which formulated the modern theory for calculating the threshold. This approach is commonly called diffusion theory, and consists of solving the continuity equation for the electron number density of the particular geometry in question, using the proper source (impact ionization) and loss terms (diffusion and attachment) corresponding to the gas in use. The culmination of the research using this theory was the publication of a book by MacDonald in 1966 [6], which quickly became the standard reference in the field. MacDonald had been involved mainly in research about the diffusion dominated microwave breakdown that occurs in the low pressure environment of ballistic missiles and space vehicles during reentry, and the practical guidelines in his book are mainly devoted to those types of situations.

The threshold for electrical breakdown in gases has a marked pressure dependence. For high pressures the threshold is rather high, and by decreasing the pressure one decreases the threshold. We will see later that it is not actually the gas pressure which is important, but rather the density. Consequently, by keeping the pressure constant while increasing the gas temperature, the threshold goes down in the same way as by decreasing the pressure. At sufficiently low pressures, a minimum threshold is reached. This point is called the Paschen minimum (from Paschen's pioneering work on DC discharges between parallel plates in 1889 [7]), and by decreasing the pressure further, the breakdown threshold again starts to rise. This is due to the fact that energy absorption by the electrons becomes less effective, and the diffusion losses to surfaces starts to become strong. Naively one might think that by approaching vacuum, the breakdown threshold goes towards infinity. Unfortunately it does not. Instead a quite different discharge mechanism starts to become important, that of multipactor (or multipaction). The multipactor phenomenon is due to electrons moving in an oscillating electric field, making impacts with surfaces and causing sec-

ondary emission of electrons. If the energy of the electrons is sufficiently high, an average net increase in the electron number will occur during impacts, and an exponential increase in the number of free electrons will take place.

An often quoted reference in the context of multipactor is the article by Farnsworth [8]. His work was devoted to the use of electron multiplication due to multipactor for the purpose of current amplification in an early form of television. Actually, in the first half of the 20th century, multipactor was only considered for beneficial uses, and it was in the context of the first satellites that it was realized to be a serious problem. A typical satellite works in an environment that is near vacuum, and it is desirable to have as high a power as possible in the transmission system, to ensure the rapid transmission of data to the earth's surface. This makes multipactor a big problem. The direct effects of multipactor are typically not very destructive to the transmission system, and will mainly result in noise and the generation of unwanted harmonics. But the deposition of energy in the system walls due to electron impact might lead to outgassing and subsequent gas discharges, which can be quite destructive.

Chapter 3

Electron motion

3.1 Introduction

To gain an understanding of the basic processes in gas discharges in general, and how to calculate the breakdown threshold, it is necessary to have a grasp of the motion of electrons under the action of electric fields and collisions with gas molecules. In this chapter we shall therefore investigate the average motion of electrons in the framework of classical physics that was first proposed by Lorentz [9], and developed for discharge purposes by Townsend [2].

3.2 Drift, collisions and energy

It is a rather curious and fortunate fact that the motion of an average electron in a gas with a low degree of ionization can be described quite well by a very simple equation

$$m\dot{\bar{u}} = -e\bar{E} - m\nu_m\bar{u} \tag{3.1}$$

where m is the electron mass, $\bar{u}$ the average electron velocity, dot denotes differentiation with respect to time, e is the electron charge, $\bar{E}$ the electric field, and ν_m the effective frequency for momentum transfer.

The electric field imparts a force on the electron, and would it not be for collisions the electron would move strictly along the field lines. Collisions with gas atoms and molecules makes the electron lose momentum in the direction it was going before impact, and the mean loss of momentum averaged over all scattering angles is described by the effective frequency for momentum transfer, ν_m. It is generally not equal to the actual collision

frequency, ν_c, and can vary between 0 and $2\nu_c$ [10]. The above equation captures the average motion of electrons, but the complete motion of a single electron is given by the superposition of the average velocity with a random thermal velocity. When the collision frequency is sufficiently high, most of the kinetic energy of the electrons will be contained in this random, thermal motion, which for moderate fields is typically many times greater than the directed drift energy of the electrons. This is the motion which is responsible for the ionizing impacts, and the diffusion of electrons, but it is not described by the above equation, and has to be treated in a different manner. The notion of a collision frequency and the effective frequency for momentum transfer is fundamental to the description of gases and plasmas, but it is a quantity which is not directly measurable. Instead one measures the drift velocity imparted to electrons in a static field. This is not easy, and devising accurate methods occupied many brilliant physicists for several decades in the beginning of the 20th century. However, the drift velocity can be measured accurately, and from this one can deduce a very important quantity called the mobility. It is easily seen from Eq. (3.1) that the drift velocity reached by an electron in a static field will be

$$\bar{v}_d = -\frac{e}{m\nu_m}\bar{E} \tag{3.2}$$

and knowledge of the field strength immediately gives the ratio $e/m\nu_m$, which is called the mobility, μ. When Townsend measured the drift velocity he found that it was basically a linear function of the electric field divided by the gas pressure, E/p. This means that $\mu \propto 1/p$, and consequently, $\nu_m \propto p$. It turns out that many important parameters are functions of E/p. By introducing an oscillating field into Eq. (3.1) we can analyze the dependence of the electron motion on pressure and frequency, and see why E/p is such an important quantity. We use $\bar{E} = \bar{E}_0 \sin\omega t$, where ω is the field radian frequency, and t is the time, and find the steady state solution for the average electron motion, $\bar{u}$, and position, $\bar{r}$,

$$\begin{aligned} \bar{u}(t) &= \frac{e\bar{E}_0}{m(\omega^2+\nu_m^2)}\left[\omega\cos\omega t - \nu_m \sin\omega t\right] \\ \bar{r}(t) &= \frac{e\bar{E}_0}{m(\omega^2+\nu_m^2)}\left[\sin\omega t + \frac{\nu_m}{\omega}\cos\omega t\right] \end{aligned} \tag{3.3}$$

The above expressions do not include the solutions for the homogeneous equation, because these are evanescent, and damped out in a time scale of the order $1/\nu_m \sim 10^{-10}/p$ s, where p is measured in Torr (for a discussion on

the collision frequency see section 4.2.2). The electric field excerts a force, $\bar{F}$, on the electrons, which performs work at a rate

$$\begin{aligned} \dot{W} = \bar{F} \cdot \bar{u} = -e\bar{E} \cdot \bar{u} = \\ = \frac{e^2 E_0^2}{2m(\omega^2 + \nu_m^2)} \left[\nu_m(1 - \cos 2\omega t) - \omega \sin 2\omega t\right] \end{aligned} \tag{3.4}$$

which has an average value, $\langle \dot{W} \rangle$, given by

$$\langle \dot{W} \rangle = \frac{\nu_m e^2 E_0^2}{2m(\omega^2 + \nu_m^2)} \tag{3.5}$$

The electrons are gaining energy from the field and constantly loosing energy from collisions with neutrals. The energy loss through elastic collisions is very small ($\sim m/M < 1/2000$), and it is the inelastic collisions that determines the steady state energy of the electrons. Inelastic collisions are mainly of the type where the electron imparts rotation and excites the neutral, but at sufficiently high energies, the electron will be able to ionize the neutral, loosing almost all its kinetic energy in the process, and releasing another electron into the gas. The average electron will loose a fraction δ_m of its energy upon making an inelastic impact. This parameter is an average over all electron energies and all possible impacts, hence it is sensitive to the gas used, and the strength of the field. Consequently, it is not possible to give one value for it, but it is somewhere around 1/100 for gas discharges in air [10].

The equation for the average energy of electrons taking into account the action of the electric field and inelastic collisions is

$$\frac{\partial \langle W \rangle}{\partial t} = \frac{\nu_m e^2 E_0^2}{2m(\omega^2 + \nu_m^2)} - \nu_c \delta_m \langle W \rangle \tag{3.6}$$

A steady state average electron energy is thus reached at

$$\langle W \rangle = \frac{\nu_m e^2 E_0^2}{2m\nu_c \delta_m (\omega^2 + \nu_m^2)} \propto \frac{E_0^2}{2(\omega^2 + \nu_m^2)} \tag{3.7}$$

where the factor 1/2 arise from the averaging of the action of the sinusoidal electric field over a period.

If we use a DC field in Eq. (3.1), we find

$$W_{\mathrm{DC}} = \langle W_{\mathrm{DC}} \rangle = -\frac{e\bar{E} \cdot \bar{v}_d}{\delta_m \nu_c} = \frac{e^2 E^2}{m\nu_m \delta_m \nu_c} \propto \frac{E_0^2}{\nu_m^2} \tag{3.8}$$

We can draw two very important conclusions. First of all, an oscillating field will impart an average energy to the electrons equivalent to that which a DC field would do if the effective field amplitude E_e is equal to the DC field amplitude. The effective field amplitude is given by

$$E_e = \frac{E_0}{\sqrt{2(1+\omega^2/\nu_m^2)}} \tag{3.9}$$

and was first used by Herlin and Brown [5] in calculating the microwave breakdown threshold. The concept of an effective field for energy transfer to the electrons is very important in that it forms a bridge between breakdown and discharges in static fields, and those in alternating and high frequency fields.

The second conclusion relates to the experimental discovery of Townsend. He found that many important parameters are functions of E/p. To see the reason for this we examine the formula above for the average electron energy in DC fields. It contains the collision frequency, which has been shown through experiments to be proportional to pressure over a wide range of the electric field strength. This means that

$$W_{\mathrm{DC}} \propto \frac{E_0^2}{p^2} \tag{3.10}$$

Of course, pressure itself is not the relevant parameter, but rather the density of neutral atoms. Early experiments were often conducted in room temperature, and there was no reason to take into account the effects of temperature. In this case, pressure is simply a constant multiplied with the neutral density, and no error is introduced by presenting the data as a function of E/p. In any case, the mean electron energy is a function of E/N, where N is the number density of the neutral gas. The electron energy is of fundamental importance for the basic processes governing the discharge dynamics, and it has been found that by plotting parameters as a function of E/p or E/N one will get universal curves, that can be used for a wide range of electric field strengths and pressures.

When one is using the data provided in the litterature, it is crucial to have an understanding of the concept of effective pressure. The data is typically presented as a function of E/p. One cannot interpret this pressure as the absolute pressure, if one is not certain that the temperature is constant. Instead it should be realized that the pressure used in this case is a constant, C_1, times the gas number density, N. We therefore have

$$p = C_1 N \tag{3.11}$$

The reference level should always be atmospheric pressure, p_0, having a number density, N_0. Thus

$$p = p_0 \frac{N}{N_0} \tag{3.12}$$

By using the ideal gas law we find that the absolute pressure, p_A, is

$$p_A = N k_B T \tag{3.13}$$

where k_B is the Boltzmann constant, and T is the temperature in K. Thus,

$$p_0 = p_A \frac{N_0}{N} \frac{T_0}{T} \tag{3.14}$$

where $T_0 = 293$ K is the room temperature. Combining Eqs. (3.12) and (3.14) we find

$$p = p_A \frac{T_0}{T} \tag{3.15}$$

By applying this formula, one can use the data given in tables and diagrams for any desired temperature that is not too high (< 2000 K for air), or too close to absolute zero. What is also of great practical importance, is that one can quickly determine how the breakdown threshold changes with temperature, simply by using formulas of the type Eq. (3.19).

3.3 Breakdown threshold in an infinite homogeneous field, and its dependence on pressure

Using the equation for the mean electron energy in an oscillating electric field we can make a qualitative assessment of the necessary field strength for breakdown in a homogeneous electric field without any bounding surfaces. In this case, breakdown will be achieved simply when the electrons have gained enough energy to ionize the neutrals at a higher rate than they succumb to capture by neutrals and ions. Since we have calculated the mean energy, it is not proper to equate this to the ionization potential. In a more detailed calculation one would find that only the high energy tail of the electron distribution function is involved in the ionization process. We can take account of this by stating that breakdown will be achieved when the mean electron energy reaches a certain fraction, f, of the ionization energy of the neutral molecules, U_i. In air, the ionization energy would correspond to that of O_2, because although the fraction of N_2 in air is higher, the ionization

energy of oxygen is lower ($U_{i,\mathrm{O}_2} = 12.2$ eV vs. $U_{i,\mathrm{N}_2} = 15.58$ eV [10]), and any electron reaching the ionization energy of oxygen will rapidly loose it due to an ionizing impact. The breakdown threshold, $E_0 = E_b$, can then be evaluated by setting $\langle W(E_b)\rangle = fU_{i,\mathrm{O}_2}$, and using Eq. (3.7), which means

$$\langle W\rangle \approx fU_{i,\mathrm{O}_2} \quad \Leftrightarrow \quad E_b \approx \sqrt{\frac{2m\nu_c\delta_m(\omega^2+\nu_m^2)fU_{i,\mathrm{O}_2}}{\nu_m e^2}} \propto \sqrt{\omega^2+\nu_m^2} \tag{3.16}$$

So for low pressures, $\omega \gg \nu_m$, the breakdown field seems to be independent of pressure, and approaches

$$E_b(\omega \gg \nu_m) \sim \omega\sqrt{\frac{2m\nu_c\delta_m fU_{i,\mathrm{O}_2}}{\nu_m e^2}} = C_2\omega \tag{3.17}$$

For high pressures, $\omega \ll \nu_m$, the electric field is proportional to the collision frequency, and consequently proportional to the effective pressure.

$$E_b(\omega \ll \nu_m) \sim p\frac{\nu_{m,0}}{p_0}\sqrt{\frac{2m\nu_c\delta_m fU_{i,\mathrm{O}_2}}{\nu_m e^2}} = C_3 p \tag{3.18}$$

This is indeed what one finds when measuring the breakdown threshold for high pressures. In air, the simple formula [6]

$$\frac{E_e}{p} \approx \frac{E_0/\sqrt{2}}{p} \approx 32 \ \ \mathrm{V/cm \cdot Torr} \tag{3.19}$$

gives an estimate for the breakdown threshold at pressures higher than the Paschen minimum. For pressures lower than the Paschen minimum, the breakdown field rises with decreasing pressure. This is contrary to the prediction of Eq. (3.17), and the reason is that in any experiment, the discharge will occur in a finite volume, and electron drift and diffusion out of this volume becomes an important electron loss mechanism when pressures get lower. The qualitative form of the breakdown threshold is shown in Fig. 3.1. In chapter 4 we shall dive deeper into the theory on how to calculate the gas breakdown threshold for different systems.

3.4 The vacuum limit

Naively, one might think that by completely removing the gas, breakdown becomes impossible. Unfortunately, this is not the case. For high frequency

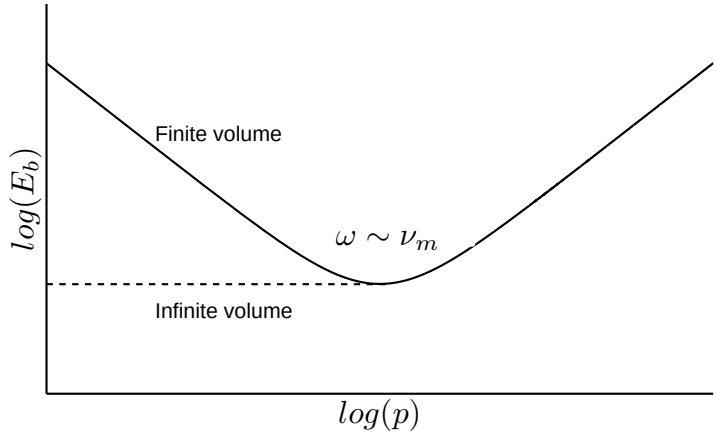

Figure 3.1: The qualitative appearance of the microwave gas breakdown threshold in a homogeneous electric field. The transition between the low and high pressure regions takes place around $\omega \sim \nu_m$. The dashed line represents the theoretical case of an infinite breakdown volume, whereas the solid line represents what one would see in a actual experiment.

applications, multipactor becomes a great risk, and even for DC conditions one might run the risk of breakdown through what is called vacuum arcing. The problem of vacuum arcing arises mainly in connection with accelerators, where very high static electric fields causes field emission and other complicated phenomena, ultimately leading to breakdown. Our main concern in this thesis is with microwave fields, and the multipactor discharge is fortunately far simpler to describe. The basic mechanism of multipactor involves the impact and secondary emission of electrons on conducting or dielectric surfaces. A necessary criterion for a discharge to develop is a sufficient field strength to energize the electrons enough to cause a net increase in their number due to secondary emission. It is also necessary to have an oscillating electric field. Otherwise any emitted electrons will be accelerated back to the surface and be absorbed.

Mainly due to historical reasons, a third criterion has attracted a lot of interest, and continues to do so; that of resonant electron motion. This criterion is based upon the assumption that the entire electron motion is dictated by the electric field. This means that for an avalanche to develop between two conducting surfaces, an electron has to strike the opposing surface at the correct time with respect to its time of emission. This criterion leads to a set of clearly separated resonance bands, outside which multipactor should

be impossible. This is true enough for small structures, where electrons are able to traverse the critical gaps in a few field cycles. But for larger structures, the thermal spread in emission velocity causes the resonance zones to blur, and makes the last criterion meaningless.

The motion of electrons in vacuum is described by Eq. (3.1) without the collision term. We use an electric field on the form $\bar{E} = \bar{E}_0 \sin \omega t$, and consider an electron that is emitted from a surface at $\bar{r} = 0$, into vacuum at a time t_e, with an initial velocity $\bar{v}_e$. The electron motion is then determined by

$$\begin{aligned} \bar{v}(t) &= \frac{e\bar{E}_0}{m\omega} \cos \omega t + \bar{v}_e - \frac{e\bar{E}_0}{m\omega} \cos \omega t_e \\ \bar{r}(t) &= \frac{e\bar{E}_0}{m\omega^2} \left[\sin \omega t - \sin \omega t_e\right] + \left[\bar{v}_e - \frac{e\bar{E}_0}{m\omega} \cos \omega t_e\right] (t - t_e) \end{aligned} \tag{3.20}$$

The most interesting point to be made about the equations above is the fact that the electron acquires a drift velocity, $\bar{v}_d$, and an oscillatory velocity, $\bar{v}_{\text{osc}}$, given by

$$\bar{v}_d = \bar{v}_e - \frac{e\bar{E}_0}{m\omega} \cos \omega t_e \tag{3.21}$$

and

$$\bar{v}_{\text{osc}} = \frac{e\bar{E}_0}{m\omega} \cos \omega t \tag{3.22}$$

where $\bar{v} = \bar{v}_{\text{osc}} + \bar{v}_d$.

Thus, the drift velocity is determined by the emission time, t_e, and the emission velocity, which is a characteristic of the material in question and the impact energy. It is clear that the maximum velocity with which the electron can impact another surface is

$$v_{\max} = v_e + 2\frac{eE_0}{m\omega} \tag{3.23}$$

The energy of an impacting electron is deposited in the surface, exciting electrons, creating vibrations in the atomic structure and so on. If the impact energy is high enough, an electron in the immediate impact region might accuire enough energy to overcome the potential barrier of the surface, given by the work function of the material in question, and be emitted as a secondary electron. For even larger impact energies, several electrons might be emitted. Obviously, the probability of all the impact energy being

imparted to one secondary electron is rather small, and the necessary maximum impact energy to create a secondary must be several times the work function of the material. So the first criterion for multipactor is that the maximum impact energy is some constant, $C_4 > 1$, times the work function of the material, W_{surf}

$$\frac{1}{2}mv_{\text{max}}^2 > C_4 W_{\text{surf}} \quad \Leftrightarrow \quad E_0 > \frac{m\omega}{2e}\left[\sqrt{\frac{2C_4 W_{\text{surf}}}{m}} - v_e\right] = C_5(v_e)\omega \quad (3.24)$$

This formula is very reminiscent of the breakdown criterion in a low pressure gas in a homogeneous field that we derived earlier (Eq. (3.17)). The breakdown field scales as ω, but in this case, there is an influence from the emission velocity, which is a stochastic variable, normally assumed to have a Maxwellian distribution. In the case of gas breakdown, any effect of initial velocities of the electrons is rapidly destroyed through collisions.

If we incorporate this threshold into the previous diagram, Fig. 3.1, we get a universal curve for microwave breakdown. The transition from gas breakdown to multipactor appears in the pressure region where the mean free path of electrons, l, is of the same order of magnitude as the system dimensions, L. The qualitative behavior of the microwave threshold for the full range of pressures is shown in Fig. 3.2. In chapter 5 we shall explore different ways of how to accurately determine the threshold for multipactor breakdown.

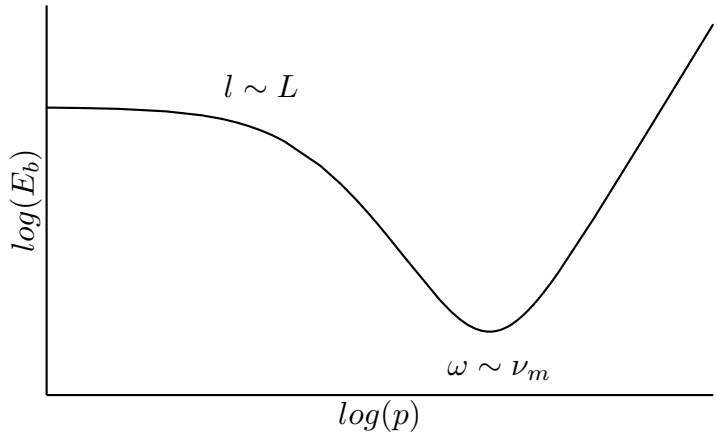

Figure 3.2: The qualitative appearance of the microwave breakdown threshold including both multipactor (vacuum) and the gas breakdown range. The transition between multipactor and corona takes place around $l \sim L$. The finer details of this transition region are not included [11].

Chapter 4

Microwave corona breakdown

4.1 Introduction

The average electron theory presented in section 3 is the simplest approach out of three possible ways to attack the problem of electron motion under the influence of collisions with neutral gas molecules. The two more sophisticated options being: kinetic theory, where the electron population is described by a continuous velocity distribution; and single particle theory, where the position and velocity of each electron is tracked. The latter approach is feasible for smaller systems, where the particles number perhaps a few thousand, but for realistic conditions (10^{19} particles per cm^3 at atmospheric pressures) it becomes impractical. So if we wish to calculate breakdown thresholds in realistic systems we have to use kinetic theory.

4.2 Diffusion theory

4.2.1 Kinetic theory, velocity moments, and the diffusion theory

The fundamental assumption of kinetic theory is that a gas is composed of a huge number of particles, and by assuming some properties for these particles, and considering their motion, the macroscopic observable properties of the gas can be derived. In the beginning of the 20th century this was still a controversial hypothesis, but nowadays it is generally acknowledged that gases consists of atoms and molecules in perpetual thermal motion.

In the case of partially ionized gases one should consider the dynamics of neutral molecules and electrons, while being accelerated by the electric and magnetic fields, and undergoing collisions with each other. To describe the basic properties of the gas it is generally sufficient to consider the motion of electrons, and assume that the neutral molecules form a static background. This is justified by the fact that the electron mass is three orders of magnitude smaller than the molecule mass. Under thermal equilibrium this leads to electron velocities which are at least 50 times higher than the gas molecule velocities. Add to this the fact that under breakdown conditions, the electrons are not in thermal equilibrium with the gas, but instead we have a situation where electrons receive energy from the electric field, which they loose mainly through inelastic collisions with neutrals. These collisions are the only heating source for the neutrals, and for low pressures, it will not lead to any substantial thermal agitation of the gas.

To treat this huge number of electrons mathematically, one introduces a distribution function, $f(\bar{v}, \bar{r}, t)$. The distribution function contains information about the density of electrons in velocity, $\bar{v}$, and configuration space, $\bar{r}$, as a function of time, t. By taking appropriate integrals of the distribution function one can find the actual electron density at a certain point in space, n, as well as average electron velocity, $\bar{u}$, and other quantities.

$$n(\bar{r}, t) = \int_{-\infty}^{\infty}\int_{-\infty}^{\infty}\int_{-\infty}^{\infty} f(v_x, v_y, v_z, x, y, z, t)dv_x dv_y dv_z = \int_{-\infty}^{\infty} f d^3v \quad (4.1)$$

$$\bar{u}(\bar{r}, t) = \frac{1}{n}\int_{-\infty}^{\infty} \bar{v} f d^3v \quad (4.2)$$

We can transform to polar coordinates in velocity space ($v_x = v\sin\theta\cos\phi$, $v_y = v\sin\theta\sin\phi$, and $v_z = v\cos\theta$), and for an isotropic velocity distribution, the density integral reduces to

$$n(\bar{r}, t) = 4\pi\int_0^{\infty} f(v)v^2 dv \quad (4.3)$$

whereas the average velocity is zero.

To find the distribution function, it is necessary to solve the Boltzmann equation

$$\frac{\partial f}{\partial t} + \bar{v}\cdot\frac{\partial f}{\partial \bar{r}} - \frac{e}{m}(\bar{E} + \bar{v}\times\bar{B})\cdot\frac{\partial f}{\partial \bar{v}} = \frac{df}{dt}|_{\text{coll}} \quad (4.4)$$

where the evolution of the distribution function is dictated by the influence of electric and magnetic forces as well as collisions. To the unaccustomed eye,

this equation looks extremely complicated, and indeed, it often is. Especially since one has to solve the Maxwell equations simultaneously to retrieve the electric and magnetic fields. The most problematic term however is found on the right hand side, where collisions of all types are symbolized by a derivative - the collision operator. The actual form of the collision operator depends on the gas, but in general it should include both elastic and inelastic collision processes. This makes it an integral over all velocity space, and general solutions are rather hard to find.

For some of the noble gases, the collisional properties are well known and not too complicated. Therefore, it is possible to find quite accurate solutions for the breakdown threshold in homogeneous electric fields that are not too strong. For the HeG gas (helium with a small admixture of mercury) it is actually possible to calculate the breakdown threshold analytically using hypergeometric functions [6], but for the more complicated gases, especially air, the number of different types of collisions becomes overwhelming. Lacking precise data for each type of collision, the correct evaluation of relevant quantities becomes very hard.

However, it is not necessary to solve the Boltzmann equation to find a good estimate for the breakdown threshold. Instead one can work with the fluid equations derived from the Boltzmann equation while using empirical values for the macroscopic parameters [1], such as ionization and attachment frequency. This method was introduced by Herlin and Brown [5] and has proven to work very well.

By taking velocity moments of the Boltzmann equation [2] one obtains a set of simpler equations, where the electron density and average electron velocity is influenced by macroscopic parameters. The first two velocity moments yields the continuity and momentum equations respectively

$$\frac{\partial n}{\partial t} + \nabla \cdot (n\bar{u}) = S_e - L_e \tag{4.5}$$

$$mn(\frac{\partial \bar{u}}{\partial t} + (\bar{u} \cdot \nabla)\bar{u}) = -\nabla p_e - en(\bar{E} + \bar{u} \times \bar{B}) - mn\nu_m \bar{u} \tag{4.6}$$

[1] In the context of kinetic theory, the term macroscopic refers to an average over velocity space. For example: temperature is a macroscopic variable which measures the average random kinetic energy of the particles, and hence the energy content of the gas, whereas the concept of temperature for a single particle is rather pointless, and it is better to speak of the microscopic, stochastic variable velocity.

[2] The proceedure of taking moments consists of multiplying with a variable and integrating over velocity space. The proceedure for finding the first couple of velocity moments can be found in any standard text on kinetic theory or plasma physics.

The letters S_e and L_e refers to a source of electrons (ionization) and a loss of electrons (attachment and recombination), which we will discuss later. The electron pressure, p_e, should not be confused with the effective pressure introduced earlier. Now we assume that the magnetic field, $\bar{B}$, is quite weak (which is true for most microwave transmission devices), and that the drift velocity, $\bar{u}$, is rather small, or equivalently that the collision frequency, ν_m, is very large. Then the momentum equation (4.6) reduces to

$$\bar{u} = -\frac{e}{m\nu_m}\bar{E} - \frac{\nabla p_e}{nm\nu_m} \tag{4.7}$$

We recognize the factor in front of the electric field as the mobility, $\mu = e/(m\nu_m)$, which can be measured in experiments. By using the ideal gas law, $p_e = nk_BT_e$, we can write

$$\bar{u} = -\mu\bar{E} - \frac{1}{n}\nabla(\frac{k_BT_e}{m\nu_m}n) \tag{4.8}$$

which by introducing the diffusion coefficient, $D \equiv k_BT_e/(m\nu_m)$, can be written as

$$\bar{u} = -\mu\bar{E} - \frac{\nabla(Dn)}{n} \tag{4.9}$$

The diffusion coefficient is a measure of the speed at which electrons will move out from regions of high concentration simply due to random motion. D is of course also a macroscopic parameter which has to be measured in experiment, or derived in a more careful way from kinetic theory [6]. If we insert Eq. (4.9) into Eq. (4.5) we get

$$\frac{\partial n}{\partial t} = \nabla\cdot(n\mu\bar{E} + \nabla(Dn)) + S_e - L_e \tag{4.10}$$

The source and loss terms can be approximated by using effective rates of ionization, $n\nu_i$, attachment, $n\nu_a$, and recombination, $\alpha_r n^2$, which finally leads to [3]

$$\frac{\partial n}{\partial t} = \nabla\cdot(n\mu\bar{E} + \nabla(Dn)) + n(\nu_i - \nu_a) - \alpha_r n^2 \tag{4.11}$$

This equation is valid for a wide range of situations in the context of gas discharges. When dealing with high electron densities, it is also necessary

[3] Sometimes an electron loss by convection of the bulk gas is included. This term is for instance very important when dealing with antennas mounted on supersonic vehicles and such [12, 13], but we choose not to include it in our studies.

to take into account the effect of the electrons on the electromagnetic field. If we are only interested in finding the breakdown threshold, such considerations are unnecessary, and as we will see later, one does not need to take account of the recombination rate, since it only becomes important at high densities. Furthermore, when the frequency of the electric field is high, the effect of mobility drift of electrons becomes small, and depending on the system size, it is almost always possible to neglect the electron drift when calculating the breakdown threshold in microwave fields. With the above assumptions, we end up with

$$\frac{\partial n}{\partial t} = \nabla^2(Dn) + n(\nu_i - \nu_a) \tag{4.12}$$

In principle, this is the equation which was introduced by Herlin and Brown [5] (although at that time they did not include attachment), which has since then been the starting point for almost all attempts at determining the microwave breakdown threshold.

The breakdown threshold for a continuous wave (CW) field is defined as the point where the electron density does not change in time, i.e. $\partial n/\partial t = 0$. At this point, the electron production and loss rates are balanced, and the electron density remains constant or zero. A minute increase in the production rate leads to an exponential increase in the electron density, whereas a small decrease in the production rate leads to exponential decay.

Finding the microwave breakdown threshold then consists of solving

$$\nabla^2(Dn) + n(\nu_i - \nu_a) = 0 \tag{4.13}$$

After all the trouble we have gone through in deriving Eq. (4.13), one might think this to be an easy task. Unfortunately, it is not. The diffusion coefficient as well as the ionization and attachment frequencies are different for all gases, and functions of the electric field strength and gas pressure. They have to be determined from careful experiments and calculations, and as we shall see, finding the correct data is hard.

4.2.2 Collision frequency

In partially ionized gases at intermediate pressure, the main collision type for electrons is the elastic electron-neutral collision. In such a collision the electron energy loss is of the order m/M, where m is the electron mass, and M the mass of the neutral molecule. Since the electrons loose so little energy, but their direction of motion is thrown off, the electrons are able to gain energy from moving in the electric field, which in turn enables the

electron avalanche. The collision rate can be found from considering the risk of collision for an electron moving in a straight line in a tenuous cloud of spherical molecules with cross sectional area σ_N, and number density N. The probability of collision while traversing a small distance Δx is $N\sigma_N\Delta x$. Thus the probability for an electron to suffer collision at x, after having travelled a distance $x - \Delta x$ without any collisions, is $p(x)\Delta x$, where

$$p(x) = N\sigma_N(1 - N\sigma_N\Delta x)^{x/\Delta x - 1} \tag{4.14}$$

Letting $\Delta x \to 0$, and using the definition of the number e, one finds

$$p(x) \approx N\sigma_N \exp(-N\sigma_N x) \tag{4.15}$$

which allows us to calculate the mean free path, l, as

$$l = \langle x \rangle \approx \int_0^\infty xN\sigma_N \exp(-N\sigma_N x)dx = 1/(N\sigma_N) \tag{4.16}$$

The most important feature of this result is that the mean free path is inversely proportional to the gas density. We can also find the collision frequency, ν_c, for an electron moving with speed v, as

$$\nu_c \approx \frac{v}{l} \approx v\sigma_N N \tag{4.17}$$

The collisional cross section for air can be measured in experiments, and for electron energies in the breakdown range, it is basically constant. However, the nature of the collision process can vary between grazing impacts, and head on impacts. The relevant quantity with regards to the mean momentum loss is thus the effective collision frequency for momentum transfer, $\nu_m(v)$. It is a function of the electron velocity, but since the main part of the electron distribution function is almost independant of the electric field in the breakdown range, it is typical to use an average value for the collision frequency which is independent of the electric field strength. Raizer gives a value of [10]

$$\frac{\nu_m}{p} \approx 3.9 \times 10^9 \quad \text{s}^{-1}\text{Torr}^{-1} \tag{4.18}$$

for E_e/p in the range of 4 to 50 V/(cm· Torr). MacDonald [6] derived an average value which is approximately valid in the typical breakdown range. He assumed a Maxwellian electron velocity distribution and found

$$\frac{\nu_m}{p} \approx 5.3 \times 10^9 \quad \text{s}^{-1}\text{Torr}^{-1} \tag{4.19}$$

This is the standard approximation used in almost all publications on microwave breakdown in air.

4.2.3 Ionization and attachment rates

Electron impact ionization is the process where a high energy ($\sim$ 10 eV) electron collides with a neutral gas molecule, looses most of its kinetic energy to the molecule, which then ejects its outer electron and forms a positive ion. The ejected electron will in turn be accelerated by the electric field and itself undergo ionizing coliisions. This is the basic mechanism which drives the electron avalanche. While an electron moves under the action of the electric field, it will undergo many collisions with neutral molecules. Most of these collisions are elastic, and the electron retains most of its kinetic energy, but undergoes a shift in its direction of motion. This is the mechanism by which electrons are able to gain energy from the field. Some of these collisions will be inelastic, and the electron may loose most of its energy while imparting rotation to the neutrals, exciting them, ionizing them etc. But in certain gases, there is also the possibility of the electron sticking to the neutral, and forming a negative ion. This process is called attachment, and occurs in the so called electronegative gases (e.g. O_2, H, SF_6 [10, 14]). The immediate effect of attachment is the effective removal of an electron from the avalanche process, since the negative ion that is formed is too heavy to play any significant role, and although the electron will eventually deattach from the molecule, the time-scales for such events are in general far longer than the typical time-scale for the avalanche process. This makes attachment the most important (along with diffusion) electron removal process for those gases where it occurs. In air under breakdown conditions, the most important attachment process is the disassociation of an oxygen molecule, $e+O_2 \rightarrow O^-+O$ [15]. The gas SF_6 has a very high attachment rate and is therefore used in certain high power devices where breakdown is unwanted. On the other hand, the gases where attachment is absent (e.g. the noble gases helium, neon and argon) are relatively easy to ionize, and frequently used when one whishes to create a plasma.

In order to use Eq. (4.13) we need some sort of mathematical expression for the ionization and attachment rates. Since these processes are heavily dependent on the electron energy, it is likely that they should be functions of E_e/p, on the form [4]

[4]The fact that it is the $\nu_{i,a}/p$ and not $\nu_{i,a}$ that shows a similarity relationship with respect to E_e/p might seem intuitively correct, for in some sense it should represent the ionization/attachment frequency per neutral molecule, but in reality, it is simply an

$$\frac{\nu_{i,a}}{p} = f(\frac{E_e}{p}) \quad \mathrm{s}^{-1}\mathrm{Torr}^{-1} \tag{4.20}$$

When searching for such formulae in the litterature, one is struck by the bewildering number of different expressions. Woo and Degroot [16] use

$$\begin{aligned} \frac{\nu_i}{p} &= 5.14 \times 10^{11} \exp(-73(\frac{E_e}{p})^{-0.44}) \\ \frac{\nu_a}{p} &= 7.6 \times 10^{-4}(\frac{E_e}{p})^2(\frac{E_e}{p} + 218)^2 \end{aligned} \tag{4.21}$$

while Taylor et al. use [17]

$$\frac{\nu_i - \nu_a}{p} = 4 \times 10^7(\frac{E_e}{100p})^{5.33} - 6.4 \times 10^4 \tag{4.22}$$

and Fante et al. use [18]

$$\begin{aligned} \frac{\nu_i}{p} &= 8.35 \times 10^{-4}(\frac{E_e}{p})^{5.34} \\ \frac{\nu_a}{p} &= 6.4 \times 10^4 \end{aligned} \tag{4.23}$$

These are only a few of the expressions one might find when perusing the litterature, and there are certainly many others (e.g. [19–21]). Looking at the different formulas, a number of questions arises. Why are there so many different approximations, and why is the attachment frequency sometimes presented along with the ionization frequency? It turns out that it is very hard to measure the microwave ionization and attachment frequencies directly. One technique uses short pulses of microwaves [22], this virtually eliminates diffusion losses, and by using Eq. (4.12) to express the electron density after the pulse time, τ

$$n(\tau) = n_0 \exp((\nu_i - \nu_a)\tau) \tag{4.24}$$

one can find the ionization and attachment rates by

$$\nu_i - \nu_a = \frac{\log(n/n_0)}{\tau} \tag{4.25}$$

experimental fact.

Besides the fact that this technique relies on the accurate measurement of n, and knowledge about the ambient electron density (mainly produced by cosmic rays), there is no way to separate the ionization and attachment frequencies from each other. A complementary technique assumes that the diffusion rate is rather well known and can be described by a characteristic diffusion length, Λ, i.e.

$$\nabla^2(Dn) \to -\frac{D}{\Lambda^2}n \tag{4.26}$$

giving

$$\nu_i - \nu_a = \frac{\log(n/n_0)}{\tau} + \frac{D}{\Lambda^2} \tag{4.27}$$

Needless to say, this technique will only be as accurate as the knowledge about the diffusion rate, and again, the ionization and attachment rates cannot be separated.

There is however a more popular technique for obtaining the frequencies. In section 3.2 we saw that DC data can be used for microwave situations by employing similarity relationships and the effective field strength, E_e. Townsend [2] measured the number of ionization events per cm the electrons travelled between electrodes. This quantity is now called the Townsend first ionization coefficient, α_i, and is a function of the DC field strength and the effective pressure

$$\frac{\alpha_i}{p} = f(\frac{E_0}{p}) \quad \text{cm}^{-1} \tag{4.28}$$

By multiplying (4.28) with the drift velocity, v_d, we find the ionization frequency

$$\frac{\nu_i}{p} = \frac{\alpha_i}{p}v_d = \frac{\alpha_i}{p}\mu E \tag{4.29}$$

There is big problem though: Townsend failed to separate ionization and attachment, and again we have found the combined, net ionization frequency. All the measurements at this time only measured the net frequency, and in addition to this, the early measurements were contaminated with mercury gas, which leads to higher ionization rates than for pure air [3, 4]. The modern measurements that most authors use are due to Harrison and Geballe [23] (the data is reproduced in [24]). They separate ionization from attachment, and use η for the number of attachment events per cm. Thus, the ionization and attachment frequencies can be found by

$$\frac{\nu_i}{p} = \frac{\alpha_i}{p}\mu E \qquad (4.30)$$
$$\frac{\nu_a}{p} = \frac{\eta}{p}\mu E$$

There is small fundamental problem associated with this proceedure. Applying DC data for microwave purposes simply by exchanging the DC field, E_0, for the effective field, E_e, is not strictly accurate. The mean energy of the electron population is the same, but the shape of the electron distribution function is not. In a DC discharge, the electron distribution function is of the Druyvesteyn form [10, 25], whereas in a microwave discharge, they should assume the Maxwellian form [10]. The error introduced by this transition should not be too great though, and most authors never mention anything about it. A much greater problem is the fact that measurements of the attachment rate, η, by other researchers show great discrepancy with Harrison and Geballe. Apparently, it is very hard to obtain correct measurements. Price [4] made a heroic attempt to bring clarity into this issue, and as to which were the most accurate measurements, but it seems impossible to determine at this moment. Instead, his recommendation was to use the combined, net ionization frequency, $\nu_{\text{net}} \equiv \nu_i - \nu_a$. In any case, the reason for the multitude of formulas is simply that researchers have calculated the ionization and attachment frequencies using different sets of DC data, and then applied curve fitting techniques. In fact, using Eqs. (4.21), (4.22) and (4.23) to calculate the high pressure threshold (i.e. equating ionization and attachment frequencies) gives a value at $E_b/p \approx 30$, which is lower than the standard value $E_b/p \approx 32$. The reason for this is likely the need for compromise between finding a simple formula to fit to the curve, while trying to be as accurate as possible. In any case the notion of calculating an exact value for the breakdown threshold is unrealistic. Any experiment will suffer from local variations in humidity, contamination, air composition etc. The point of calculating a threshold is rather to give an upper margin for the allowable power, and then to keep a safe distance to that margin.

In papers A and B we used Eq. (4.22) when calculating the breakdown threshold for some different geometries.

4.2.4 Diffusion

Diffusion is the process where spatial inhomogeneities in a particle distribution are reduced simply through the random motion of the particles. This

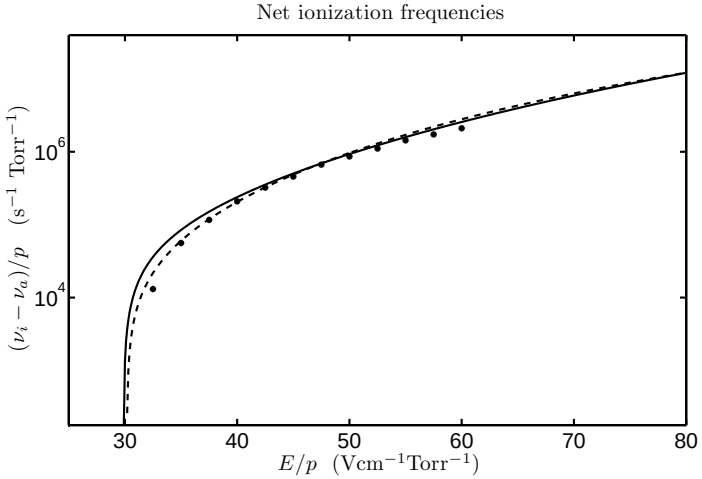

Figure 4.1: A comparison between the net ionization rate given by Eqs. (4.21) (dashed line) and (4.22) (solid line), and calculated from the data of Harrison and Geballe [23] (reproduced in [24]) using a curve fit by for the drift velocity by Price [4] to the data of Townsend and Tizzard [27].

type of problems are typically called random walk, or Brownian motion. In section 4.2.1 we defined the diffusion coefficient as

$$D = \frac{k_B T_e}{m\nu_m} \tag{4.31}$$

By using the mobility, $\mu = e/(m\nu_m)$, one can write the above formula as

$$\frac{\mu}{e} = \frac{D}{k_B T_e} \tag{4.32}$$

which is called the Einstein relation, and connects diffusion with mobility. It was originally found by Einstein in his investigation on Brownian motion. For us to be able to use the formulas previously derived to calculate the breakdown threshold, we need to find an expression for the diffusion coefficient. It is not easy to measure the coefficient directly through experiment, but it can be derived using knowledge about the energy spectrum of the electrons along with the collision frequency. If we assume an isotropic electron distribution in velocity space (of course, since the electric field points in a certain direction, the distribution will not be completely isotropic, but for relatively weak fields, the correction is small), the mean electron energy is connected to the temperature through (see any standard text on statistical mechanics)

$$\frac{1}{2}mv_{th}^2 = \frac{3}{2}k_B T_e \tag{4.33}$$

where v_{th}^2 is the statistical average

$$v_{th}^2 = \frac{\int_0^\infty v^4 f dv}{\int_0^\infty v^2 f dv} \tag{4.34}$$

Inserting this into Eq. (4.31) we find

$$D = \frac{v_{th}^2}{3\nu_m} \tag{4.35}$$

However, since the collision frequency is not constant with respect to electron velocity, the correct form is actually

$$D = \frac{\int_0^\infty \frac{v^2}{3\nu_m} v^2 f dv}{\int_0^\infty v^2 f dv} \tag{4.36}$$

MacDonald [6] used this expression to derive a formula for the diffusion coefficient by assuming a Maxwellian electron energy distribution and using experimental data for the mean electron energy

$$Dp = (29 + \frac{0.9E_e}{p})10^4 \quad \text{cm/s} \tag{4.37}$$

Unfortunately, the available data at that time only extended to $E_e/p = 22$ Vcm^{-1} Torr^{-1}, and there seems to have been no attempts at deriving a more accurate formula since then.

In papers A and B we used a rough value for the diffusion coefficient, $Dp = 10^6$ cm $\text{s}^{-1}\text{Torr}^{-1}$, in order to simplify calculations and make analytical assessments possible. In Figs. 4.2, 4.4, and 4.5 it is seen that the error introduced by this simplification is rather small both for homogeneous and inhomogeneous fields. The reason for this is the insensitivity of the diffusion rate with respect to the electric field strength, whereas the ionization rate is very sensitive to the field strength.

When electron densities become high, the diffusion rate goes down. This is due to the buildup of space-charge. When fast electrons are diffusing into low density regions, the ions, being much slower, will lag behind. The field which is generated by the charge separation will retard the motion of the electrons, force the electrons and ions to move at the same rate, and severly reduce the diffusion speed of the electrons. This type of diffusion is called ambipolar, and it has the fascinating consequence that a gas discharge needs

less power to be maintained than it needs to ignite. Also, the decay time of a discharge plasma will be dictated by recombination processes, and not by the diffusive evacuation of electrons out of the discharge region, as one might expect. When considering the breakdown threshold the electrons diffuse freely and we do not need to consider ambipolar diffusion. On the other hand, if one is interested in the subsequent stages of the discharge, it is necessary to take account of this effect. This was done in paper D, where we analyzed the post-breakdown evolution of a small spherical plasma region in air.

4.2.5 Recombination

Recombination is an event where charged particles collide and form neutral particles. When turning off the ionization mechanism, this process is what typically ends the plasma state. There are several different ways in which partially ionized air recombines, but the most important one for moderate pressures and temperatures is dissociative recombination, which follows the scheme $A_2^+ + e \rightarrow A + A^*$, where A is an atom, and the asterisk denotes an excited state. The rate of this process is given by $\alpha_r n^2$, where α_r is the recombination coefficient for the gas in question. In air, the most important process is the breakup of an oxygen molecule by electron impact, and a commonly used value for the recombination coefficient is [10]

$$\alpha_r \approx 2 \times 10^{-7} \quad \text{cm}^{-3}\text{s}^{-1} \tag{4.38}$$

This means that the recombination rate becomes comparable with the attachment rate at $n = \nu_a/\alpha_r \sim 10^{14}$ cm^{-3}, for atmospheric pressures. The critical density is around $n_c \approx 10^{14}$ cm^{-3} (see 4.4.1). This means that under certain circumstances, to describe the nonlinear development of a microwave breakdown plasma it is necessary to include recombination. This was done by El-Khamy [28] when calculating the heating of a low pressure air plasma by microwaves. For a small plasma region at high pressures, the recombination rate might be completely negligable, and the electron density saturates at a level which is far below the critical density. This is the case in paper D, where a small spherical breakdown region saturates at a density where recombination is very low. In general, in the quasistatic regime, a small region of field enhancement, E, which is above the breakdown threshold, E_b, will generate a plasma patch which saturates at

$$\frac{n}{n_c} \sim \frac{\omega}{\nu_m}\frac{E}{E_b} \tag{4.39}$$

For atmospheric pressure, the condition $\nu_m \gg \omega$ is generally true, which means that $n \ll n_c$, and recombination is negligable accordingly.

So much for the nonlinear stage of the breakdown development. When calculating the breakdown threshold, the electron density is far too low for recombination to have an effect, and it is generally acknowledged that there is no need to include it in breakdown calculations.

Aside from dissociative recombination, electrons will also recombine by emitting a photon (radiative recombination), and by a three body collision, where one of the neutrals absorbs the excess energy as kinetic energy. The radiative recombination becomes important only for very high electron energies, and the three body recombination process is generally negligable for gases with low degrees of ionization and low temperature. But the presence of a solid surface on the walls of any volume which encloses a breakdown region leads to a greatly increased recombination rate close to the surface. This is simply due to the great number of atoms presented by the surface, and because of this, the electron density is typically assumed to be zero on the surface, irrespective of the surface material.

4.3 Simple solutions for the breakdown threshold

To demonstrate the basic proceedure for finding and expressing the breakdown threshold we shall investigate two simple situations. The parallel plates setup consists of two large parallel metal plates with a homogeneous microwave field between them. This is the classical experimental setup which has been used on so many occasions throughout the 20th century. In the second setup we add a small field intensification close to the surface of one of the plates. This will serve to illustrate how the breakdown threshold and the size of the breakdown region varies with the pressure and local field intensifications. We shall use the different approximations in section 4.2 and compare the results to see how large one can expect the error to be by using simplified versions of the formulae.

4.3.1 Parallel plates, homogeneous field

Due to the complicated form of the diffusion coefficient, and the net ionization frequency, there is only one analytical solution corresponding to a real breakdown situation. It is the case of breakdown between two large parallel metal plates. In this case the field will be homogeneous, and the coefficients will be constant. The continuity equation on the breakdown threshold (Eq. (4.12)) becomes

$$D\frac{\partial^2 n}{\partial x^2} + n(\nu_i - \nu_a) = 0 \tag{4.40}$$

and the boundary conditions are that the electron density is zero on the plate surface (see 4.2.5), $n(0) = 0$ and $n(d) = 0$. Formally, the solution is

$$n(x) = n_j \sin\frac{j\pi}{d}, \qquad j = 1, 2, 3... \tag{4.41}$$

where $j\pi/d = \sqrt{(\nu_i - \nu_a)/D}$. Only $j = 1$ is physically interesting, since it corresponds to the lowest value of $(\nu_i - \nu_a)/D$, and the actual value for the breakdown threshold. We then have a formula for the breakdown threshold

$$\frac{\nu_i - \nu_a}{D} = \frac{\pi^2}{d^2} \tag{4.42}$$

Actually, what we want is the electrical field strength corresponding to the breakdown threshold as a function of gas pressure and gap width. Since we have expressions (see sections 4.2.3 and 4.2.4) for the net ionization frequency ($(\nu_i - \nu_a)/p \approx h_1(E/p)$) and the diffusion coefficient ($Dp \approx h_2(E/p)$), we can find the implicit solution as

$$\frac{h_1(\frac{E}{p})}{h_2(\frac{E}{p})} \approx \frac{\pi^2}{p^2 d^2} \tag{4.43}$$

This function can be inverted numerically, and the solution for the electric field strength can be seen in Fig. 4.2.

The solution shown in Fig. 4.2 is archetypical for gas breakdown curves. It clearly shows the transition from diffusion dominated breakdown to attachment dominated. The transition is governed by the combined effect of gap width and pressure, for these two parameters determine the relative influence of diffusion. Since the diffusion losses occur on the conducting surfaces, where electrons are absorbed and immediately transported away, it is of great importance what distance an electron has to travel to be absorbed by a surface versus the distance it can go before succumbing to an attachment collision.

Although Fig. 4.2 is preferable from a theoretical point of view, it is impossible to measure E_e in experiments. What one can measure is the voltage (or better yet, the power), and in a parallel plates system, the electric field is readily found by dividing voltage with gap width. Therefore, the standard style of presenting breakdown curves is in an E vs. p chart for a given field frequency and gap width. As an example we display a set

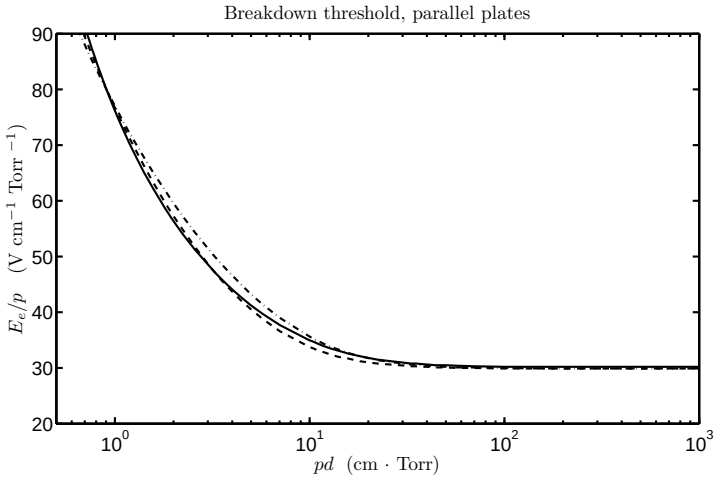

Figure 4.2: The calculated breakdown threshold in a parallel plates system using Eqs. (4.22) and (4.37) (dashed line), Eqs. (4.22) and (4.37) (solid line), Eq. (4.22) and $Dp = 10^6$ cm s^{-1} (dashed and dotted line), corresponding to the proceedure in papers A and B. The difference between the results is not too great. Note that the breakdown threshold in a large gap has the value $E_e/p \approx 30$, and not 32 V cm^{-1} as would be more accurate. This is a side-effect of the imperfect curve-fit when the formulas for the net ionization frequency were derived.

of measurements by MacDonald for a gap width of 0.69 cm, and a field frequency of 9.4 GHz. The general solution in Fig. 4.2 can be adapted to this system, and expressed in the correct variables by applying the expressions

$$p = \frac{pd}{d} \tag{4.44}$$

$$E = (\frac{E_e}{p})p\sqrt{1 + \frac{\omega^2}{\nu_m^2}} \tag{4.45}$$

$$\tag{4.46}$$

while using $d = 0.69$ cm, $\omega = 2\pi \times 9.4 \times 10^9$ s^{-1}, and $\nu_m = 5.3 \times 10^9 p$ s^{-1}. In this particular case, the factor $\sqrt{2}$ which is present in Eq. (3.9) has been removed, since MacDonald uses the root-mean-square value for the electric field.

Overall, the agreement between measured, Fig. 4.3, and calculated values, Fig. 4.4, is rather good. The slope of the curves in the high pressure region agrees fairly well, where the measured values follow $E \approx 32p$ V/cm, and the calculated $30p$ V/cm. The pressures at which the Paschen minima occur seem to be almost identical at around 8 Torr, but the measured electric field at the Paschen minimum (≈ 550 V/cm) is slightly higher as compared to the theoretical value (≈ 300 V/cm). This has to do with the inexactness of the approximations used for the net ionization frequency, and the diffusion coefficient.

4.3.2 Parallel plates with a small field inhomogeneity

If we introduce a field intensification, γ, which extends a distance $h < d$ out from one plate, the problem becomes much harder to solve using analytical and approximate analytical methods. We shall not attempt to find such a solution, but instead perform a numerical proceedure. The simplest numerical proceedure for this type of one-dimensional problems is the finite difference shooting method. If the problem is two-dimensional, as in papers A and B, the shooting method becomes unusable, and we solve those problems using basic relaxation methods.

The shooting method is the numerical equivalent of hitting the problem with a stone. One simply exchanges the exact derivatives for their discreete counterparts and express the electron density in the forward direction using the previous values. This requires that a guess is made about the value of the relevant parameters, and depending on whether the guess is good or

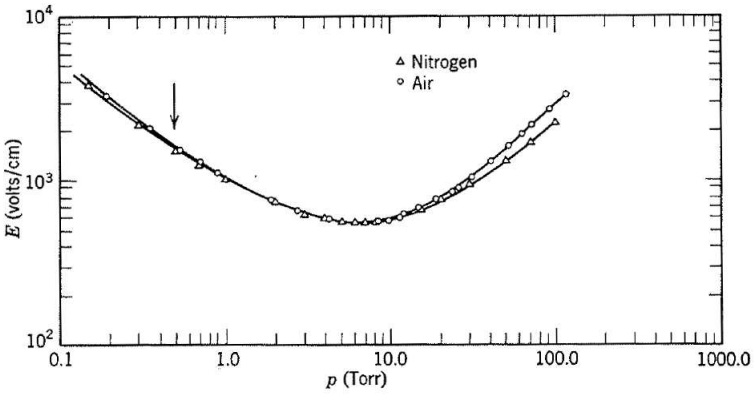

Figure A-5 Continuous-wave breakdown in air, oxygen, and nitrogen at 9.4 Gc/sec with $\Lambda = 0.22$ cm.

Figure 4.3: The measured breakdown field for air and nitrogen gas (but not oxygen as it says in the caption) in a cavity with a gap width $d = \pi\Lambda \approx 0.69$ cm, at a frequency of 9.4 GHz [6]. The qualitative behaviour of the breakdown curve agrees with the simple calculations in section 3.3, see especially Fig. 3.1.

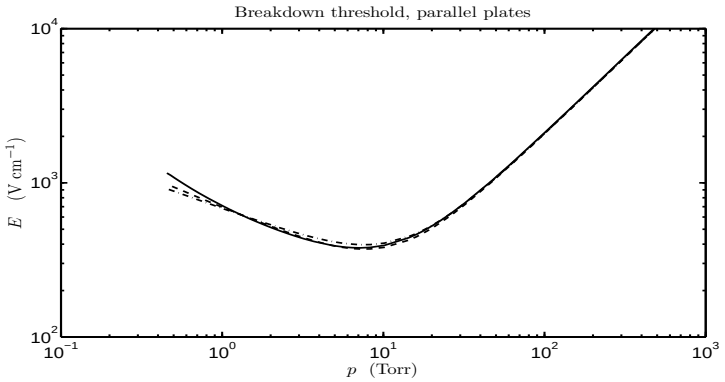

Figure 4.4: The calculated breakdown threshold for the same parameters as in Fig. 4.3. The position of the Paschen minimum depends mainly on the relative values of field and collision frequency. The fact that the position of the minimum agrees with the measured data justifies the approximate value used for the collision frequency, at least for low pressures. The divergence of the lines for low pressures has to do with the large effective field strengths and the fact that we are outside the limits of the approximate expressions in section 4.2.3.

not, the final density in the forward direction will agree with the boundary condition or not. If not, the parameters have to be adjusted. Let us look at the specific problem in more detail. We have

$$\frac{\partial^2(Dn)}{\partial x^2} + n\nu_{\text{net}} = 0 \tag{4.47}$$

with the boundary conditions $n(0) = n(d) = 0$. The first step is to normalize the x-coordinate to the gap width, i.e. $x \to x/d$, giving

$$\frac{\partial^2(Dn)}{\partial x^2} + nd^2\nu_{\text{net}} = 0 \tag{4.48}$$

with the boundary conditions $n(0) = n(1) = 0$.

A first order derivative is discretized according to

$$\frac{\partial\phi}{\partial x} = \frac{\phi(x+\Delta x) - \phi(x)}{\Delta x} + \mathcal{O}(\Delta x) \tag{4.49}$$

and a second order derivative

$$\frac{\partial^2\phi}{\partial x^2} = \frac{\phi(x+\Delta x) + \phi(x-\Delta x) - 2\phi(x)}{\Delta x^2} + \mathcal{O}(\Delta x^2) \tag{4.50}$$

Which means that our breakdown threshold equation becomes

$$\frac{n(x+\Delta x)D(x+\Delta x) + n(x-\Delta x)D(x-\Delta x) - 2n(x)D(x)}{\Delta x^2} + \\ +n(x)\nu_{\text{net}}(x)d^2 \approx 0 \tag{4.51}$$

This expression can be simplified and rearranged to yield

$$n(x+\Delta x) \approx n(x)\left[\frac{2f_1(x) - d^2p^2\Delta x^2 f_2(x)}{f_1(x+\Delta x)}\right] - \\ - n(x-\Delta x)\left[\frac{f_1(x-\Delta x)}{f_1(x+\Delta x)}\right] \tag{4.52}$$

where

$$f_1(x) = Dp = (29 + 0.9\frac{E_e(x)}{p}) \times 10^4 \quad \text{cm}^2\text{s}^{-1}\text{Torr} \tag{4.53}$$

$$f_2(x) = \frac{\nu_{\text{net}}(x)}{p} = 4 \times 10^7(\frac{E_e(x)}{100p})^{5.33} - 6.4 \times 10^4 \quad \text{s}^{-1}\text{Torr}^{-1} \tag{4.54}$$

corresponding to Eqs. (4.22) and (4.37). The proceedure now is simple, we define a vector $x[i] = (i-1)/(M-1)$, where $\Delta x = 1/(M-1)$. The electric field divided by pressure is defined as

$$\frac{E_e}{p} = \begin{cases} E_{\mathrm{e,max}}/p, & \text{if} \quad h < d \\ E_{\mathrm{e,max}}/(\gamma p), & \text{if} \quad h \geq d \end{cases} \tag{4.55}$$

When performing this type of calculations, it is a good habit to weaken the ambient field with the factor $1/\gamma$ instead of increasing the local field by the factor γ. This is to make sure that the ionization frequency in the high field region never goes above the allowed range of the expression one is using for the frequency.

Now, for a specific value for pd, one guesses a value for $E_{\mathrm{e,max}}/p$, and launches a density vector n from $i = 3$, using $n[1] = 0$, and any positive value for $n[2]$. The calculation proceeds by evaluating the forward value ($n[i+1]$) using the the backward values ($n[i]$, and $n[i-1]$), as well as the predetermined values for D and ν_{net} as a function of position i. If $n[M] = 0$, the value for the electric field divided by pressure is correct, otherwise it has to be adjusted up or down. In this way one can find the electric field through pressure as a function of pressure-gap-product, which is shown in Fig. 4.5.

4.3.3 Results, transition pressure

First of all we can conclude that it seems to make little difference if we use a constant value for the diffusion coefficient ($Dp \approx 10^6$ $\mathrm{cm^2 s^{-1}}$), or if we use the full formula given by Eq. (4.37). The reason for this is the high sensitivity of the net ionization frequency with respect to the electric field strength, as compared to the dependence of the diffusion coefficient.

Furthermore, it is also clear that if there is a small field inhomogeneity, there will be two fundamentally different regimes. For low pressures the breakdown threshold will correspond to the ambient field, and the breakdown region will be the entire gap, whereas for high pressures the breakdown threshold will be set by the intensified field and the breakdown region will be confined to this small volume. The transition takes place at the point when the attachment length is of the order of the size of the region of intensified field. The attachment length, L_a, is a measure of the typical length scale of the boundary region of a plasma [5], and is defined as

[5]The attachment length is defined by considering a one-dimensional scenario, where there is a finite region of plasma in which ionization takes place. Outside this region there is no ionization, and the plasma profile decays due to diffusion and attachment according

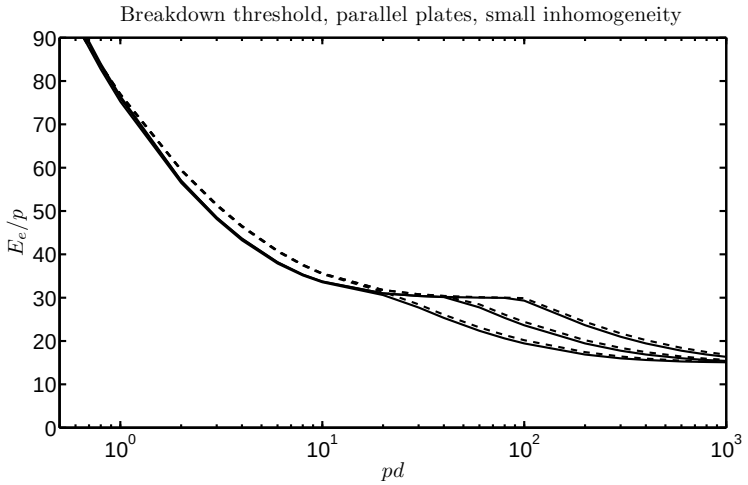

Figure 4.5: The calculated breakdown threshold in a parallel plate system with a small region of intensified field. The field enhancement factor is 2, and the three solid lines represent the results for three different sizes of the intensified region, $h/d = 0.01$, 0.02 and 0.04 from top to bottom on the right hand side of the figure. For low values of the pressure-gap product the curves are exactly the same as those for normal parallel plates. They start to digress when the attachment length is roughly equal to h. The solid curves use the variable value for the diffusion coefficient given by Eq. (4.37), and the net ionization rate Eq. (4.22), whereas the solid lines use $Dp = 10^6$ cm^2/s and Eq. (4.22).

$$L_a = \sqrt{\frac{D}{\nu_a}} \tag{4.56}$$

Of course, we already concluded that there is no good exact formula for the attachment frequency, but a simple order of estimate is what we want. For that purpose we can use $\nu_a/p \approx 6.4 \times 10^4$ s^{-1}, and $Dp \approx 10^6$ cm^2 s^{-1}. Then

$$L_a \sim \frac{4}{p} \quad \text{cm} \tag{4.57}$$

Thus, the transition takes place at

$$L_a \sim h \quad \Rightarrow \quad pd \sim 4(\frac{d}{h}) \tag{4.58}$$

Inspecting Fig. 4.5 we find the transition points where the curves display a kink. The position of these transition points agree with the order of magnitude estimate given by Eq. (4.58).

This model problem illustrates the main effect of there being a local field enhancement. It was realized long ago [29, 30] that to avoid breakdown in practical microwave systems; sharp pointy features, such as soldering points, sharp corners, metal debris etc., must be filed down or removed. Otherwise local breakdown may ensue due to the field enhancement. The importance of the size of these regions for the breakdown threshold varies greatly with pressure, and in complicated systems, the breakdown threshold might go through several different regimes under variation of the gas pressure.

4.4 Hot spots and nonlinear effects

When solving the problem of parallel plates with a small field inhomogeneity we noticed that depending on the pressure, small local field intensifications can be very important in determining the breakdown threshold. It is not immediately obvious however if the small local plasma regions created by such a breakdown will be harmful to the system. The direct effects of a very small plasma will be limited, probably resulting in some noise and minor signal reflections. But for high pressures the plasma will absorb a significant amount of microwave energy, and undergo heating, heat the surrounding gas, and consequently lower the threshold for breakdown in the surrounding

to Eq. (4.13). Solving the diffusion equation using constant values for the diffusion coefficient and the attachment frequency gives the attachment length as the length scale of the density decay.

volume. If the heating power is strong enough, the plasma may expand and eventually cause breakdown in the entire system. This is the most dangerous scenario possible, for it will most likely result in the destruction of the entire device. However, there are many other possible scenarios. Before discussing them, we shall go through the relevant physical effects.

4.4.1 Microwave absorbtion, reflection and gas heating

A region of breakdown plasma will absorb and reflect microwave energy. The amount of absorption and reflection depends on the size, shape and electron concentration of the plasma. Experimentally, one generally determines that breakdown has taken place by looking for a distinctive flash of light, listening for a snapping sound [6], or observing the sharp drop in signal transmission through the system. The signal drop comes from the reflection and absorption of microwaves. To get a basic understanding of this phenomena we shall investigate the dielectric function of a gas with a relatively low electron concentration.

Using the complex representation for the electric and magnetic fields, $\bar{E} = \Re(\bar{\mathcal{E}}\exp(i\omega t))$, and $\bar{B} = \Re(\bar{\mathcal{B}}\exp(i\omega t))$, the Maxwell equations in a weakly ionized gas can be written as

$$\nabla \cdot (\epsilon\bar{\mathcal{E}}) = 0 \tag{4.59}$$

$$\nabla \cdot \bar{\mathcal{B}} = 0 \tag{4.60}$$

$$\nabla \times \bar{\mathcal{E}} = -i\omega\bar{\mathcal{B}} \tag{4.61}$$

$$\nabla \times \bar{\mathcal{B}} = i\omega\mu_0\epsilon\bar{\mathcal{E}} \tag{4.62}$$

where

$$\epsilon = \epsilon_0\left[1 - \frac{n}{n_c}(1 + i\frac{\nu_m}{\omega})\right] \tag{4.63}$$

and $n_c = \epsilon_0 m(\omega^2+\nu_m^2)/e^2$, which is generally called the critical density. The reason for this can be seen by studying the reflection coefficient (see e.g. [31]) of a plane electromagnetic wave in vacuum (or air) incident perpendicularly on a plasma surface having electron density n

$$R = |\frac{1 - \sqrt{\epsilon/\epsilon_0}}{1 + \sqrt{\epsilon/\epsilon_0}}|^2 \tag{4.64}$$

[6] It has been observed that a shock wave accompanies the appearance of breakdown, and that sometimes this shock wave might be strong enough to crack dielectric windows and damage other equipment, but there seems to have been no serious investigation of this phenomena yet.

R represents the ratio between the reflected, S_r, and incoming energy flux, S_i. The dependence of R on n/n_c and ν_m/ω can be seen in Fig. 4.6. For low gas densities ($\nu_m \ll \omega$), the transition between low reflection and full reflection is very abrupt and occurs when the plasma frequency matches the field frequency. The field is then unable to penetrate the plasma and is totally reflected. As the gas pressure goes up, the transition becomes less abrupt, and absorption of field energy in the plasma becomes important.

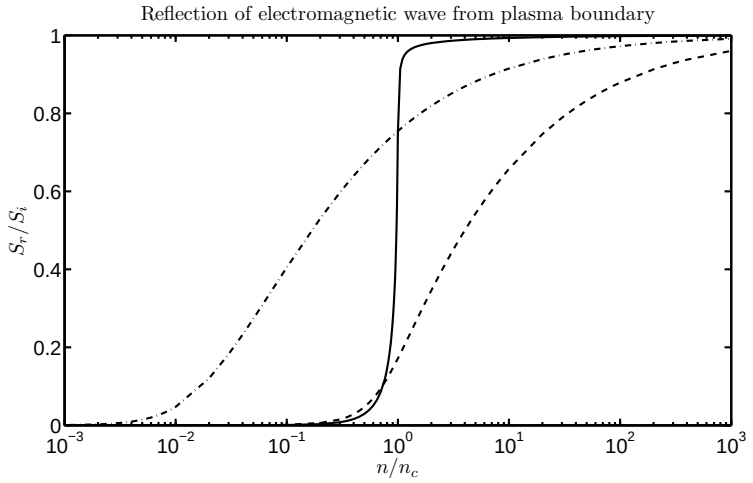

Figure 4.6: The relative amount of energy reflected from a plasma surface as a function of n/n_c for $\nu_m/\omega = 0.01$ (solid curve), 1 (dashed curve), and 100 (dashed and dotted curve). It is clear that for low values of ν_m/ω, the transition between transparent and opaque is very rapid, and very little energy is absorbed by the plasma, whereas for high values, the transition is slower, and substantial amounts of energy can enter the plasma and be dissipated within.

Approximating the refraction of an electromagnetic wave from a plasma with the case of radiation incoming on a plane surface works well when the wavelength of the field and the attachment length are much smaller than the plasma size. In a more general treatment, the transition layer between gas and plasma becomes very important. One has to take into account that the plasma itself is generated by the electric field that penetrates the plasma, and which under certain conditions will be enhanced in front of the plasma. This problem has attracted some interest, and there are a few solutions for different combinations of parameters [16, 32–34].

In the opposite case, when the plasma size is small in comparison with the wavelength, the externally applied field around the plasma can be regarded as homogeneous at any given moment in time. This is called the

quasistatic approximation. Solving the self-consistent nonlinear problem of plasma being generated by the electric field which penetrates it is still a formidable problem. For some basic structures, such as a cylindrical plasma colums, the plasma generated by two crossed beams etc., there are some rather exact solutions [35–37], but for the general problem, not much has been accomplished. In Paper D we analyze the problem of a breakdown plasma sphere in the quasistatic regime. We assume that the attachment length is small in comparison to the plasma size, which allows us to assume that the internal field is constant, and the electron density is fixed at a level which reduces the internal field to the breakdown field for that particular gas temperature. We then proceed to analyze the thermodynamical problem of heat generation within the sphere, and heat loss over the sphere edges. The solution is of a qualitative nature, since we neglect the action of the field outside the sphere created by the polarization of the plasma. A more exact treatment requires rather sophisticated computer software.

Absorption of microwaves in the plasma can also take place in different ways. If a microwave is travelling in the x-direction through a plasma, the time-averaged energy flux is described by the Poynting vector

$$\langle \bar{S} \rangle = \frac{1}{2\mu_0} \Re(\bar{\mathcal{E}} \times \bar{\mathcal{B}}^*) = \frac{1}{2\mu_0 \omega} E^2 \Re(k^*) \exp(-2\beta x) \hat{x} \tag{4.65}$$

where $k = (\omega/c)\sqrt{\epsilon/\epsilon_0} \equiv \alpha - i\beta$, and $\hat{x}$ is the unit vector in the x-direction. The dissipated energy, $\Delta\langle S \rangle$, per distance, Δx, is

$$\Delta\langle S \rangle = \frac{1}{2\mu_0 \omega} E^2 \Re(k^*)(1 - \exp(-2\beta \Delta x)) \tag{4.66}$$

The most interesting case is for high pressure gases ($\nu_m \gg \omega$), where the microwave absorption is strong. We then have

$$\alpha \approx \beta \approx \frac{\omega}{c} \sqrt{\frac{n\nu_m}{2n_c\omega}} \tag{4.67}$$

which yields

$$\Delta\langle S \rangle = \frac{1}{2\mu_0 \omega} E^2 \frac{\omega}{c} \sqrt{\frac{n\nu_m}{2n_c\omega}} (1 - \exp(-2\frac{\omega}{c} \sqrt{\frac{n\nu_m}{2n_c\omega}} \Delta x)) \tag{4.68}$$

and if the electron density is not too great ($n/n_c \ll c^2/(2\omega\nu_m)$), the field decays slowly, and we have

$$\Delta\langle S\rangle = \frac{n\nu_m e^2 E^2}{2m(\omega^2+\nu_m^2)}\Delta x \tag{4.69}$$

which is exactly what we get if we multiply Eq. (3.5) by $n\Delta x$. This is not surprising, since that formula was derived for a single electron oscillating in a homogeneous electric field.

By setting $\Delta x = 1$ cm, we find the average energy dissipation per unit volume.

$$\langle \dot{W}\rangle = \frac{n\nu_m e^2 E^2}{2m(\omega^2+\nu_m^2)} \tag{4.70}$$

The above formula can be used in the quasi-static approximation to evaluate the energy dissipation per unit volume of breakdown plasma (provided the conditions above are met) but it is necessary to find the internal field, E, from solving Maxwell's equations with a homogeneous external field. In paper D we used a well known formula for the internal field inside a dielectric sphere, $E = 3E_0/|2+\epsilon|$, where E_0 is the external field strength, along with Eq. (4.70) to evaluate the heating of a spherical region of breakdown plasma.

4.4.2 Field intensifications

In section 4.3.2 we concluded that a small field intensification may dictate the breakdown threshold for high pressures, but we never explained the cause of such an intensification. In microwave systems, field intensifications are generally caused by the mode structure of the electric field, and irregularities on the conducting surfaces. Such irregularities could for example be soldering points, sharp corners, tuning screws etc., and consequently, by smoothing out such features, the breakdown threshold for the device will be raised [29]. Other sources of field intensifications might be externally applied microwave beams, laser and such, but the discussion of such effects goes beyond the scope of this thesis.

To be more specific in how to treat the effects of surface irregularities, let us again discuss the effects of a field enhancement in the case of parallel plates, but specify that the enhancement is caused by a pointy metal feature. The shape of the point (pyramid, cone, hemisphere etc.) is highly relevant in determining the exact field enhancement factor, and the correct size of the region of enhanced field [38], but to be general we state that the field enhancement factor is γ, and the typical size of the point, and the concomitant region of enhanced field, is a. This means, that as long as $L_a \gg a$, breakdown will be achieved when the ambient effective field, E_e,

equals the breakdown threshold, E_b (where $E_b \approx 32p$ V/cm for air) at a given pressure. Whereas when $L_a \ll a$, the threshold is determined completely by the local field, γE_e, and breakdown is achieved at $\gamma E = E_b$. The approximate thresholds for breakdown as a function of effective pressure can thus be summarized (Eq. (4.57))

$$E_e = \begin{cases} E_b, & 4 \gg ap \quad \text{cm} \cdot \text{Torr} \\ \frac{E_b}{\gamma}, & 4 \ll ap \quad \text{cm} \cdot \text{Torr} \end{cases} \tag{4.71}$$

When $L_a \ll a$, the breakdown region will be completely confined to the immediate volume of the field intensification. If this volume is small, the immediate effects of the plasma will be small. Subsequent effects can vary greatly. The plasma may remain localized, expand, or even form a wave front travelling towards the microwave source. The exact response of the plasma to the TEM depends on the skin depth of the plasma, δ, in comparison to the plasma size, a, and the field wavelength, λ.

In paper B we analyze the breakdown threshold inside a cavity where a small hemispherical boss is present on one of the cavity walls. The results show quite clearly that for low pressures, the boss has a very small influence on the breakdown threshold, and breakdown in the volume would imply a plasma filling the entire cavity. For high pressures on the other hand, the breakdown threshold is completely set by the field close to the boss, and the immediate breakdown region is localized above the boss.

In paper G we analyze the situation of breakdown around a metal ball floating freely in air at atmospheric pressure. The ball is irradiated by a microwave field, which induces currents on the sphere surface, which in turn enhance the field around the ball. In the quasistatic regime, $a \ll \lambda$, where a is the ball radius, the field enhancement factor is $\gamma = 3$, whereas in the geometrical optics limit, $\gamma = 2$. This leads to the appearance of two quite different thresholds. The first and highest, E_{I}, corresponds to the equality of the external field and the breakdown field, i.e. $E_0 = E_{\mathrm{I}} = E_b$, and the immediate breakdown in the entire gas volume. The second threshold, $E_0 = E_{\mathrm{II}} = E_{\mathrm{I}}/\gamma$, corresponds to breakdown locally in the intensified field around the ball.

4.4.3 Breakdown due to heating

In section 3.2 we discussed the difference between the gas pressure and the effective gas pressure. We concluded that the determining factor for the electron energy, and the ionization rate, is the neutral gas density. Consequently, by raising the temperature, while maintaining constant pressure,

the gas density goes down, the electron energy and ionization rate go up, and the breakdown threshold is lowered. In a homogeneous field at high and moderate gas pressures (above a few Torr), using Eqs. (3.15) and (3.19), the temperature dependence of the breakdown threshold can be expressed as

$$E_b = E_{b0}\frac{T_0}{T} \tag{4.72}$$

where T_0 is the reference temperature, normaly set at room temperature, $T_0 = 293$ K.

In a situation where the field in a microwave device is below the breakdown threshold at room temperature, it is possible to instigate local breakdown by heating the gas in a specific spot. If the applied effective field is E_e, breakdown will be reached at a temperature, T_b, given by $T_b = T_0 E_{b0}/E_e$. Of course, the size of the heated region must be large enough for breakdown to develop, but exactly how large the region must be is unclear, for it involves several factors, such as the nature of the heat source, the heat loss processes, and the gas pressure.

There are several reasons why a gas might become heated locally, but a common unwanted source of heating is the presence of materials of low conductivity inside the microwave system. The device surfaces can be dirty, covered in a thin film of oil, and there can be debris of different forms; plastic, rubber, dust etc.

One can make a rough estimate of the heating of an object with low electric conductivity provided that the relative permittivity, ϵ_r, the electric conductivity, σ, and the field picture are known. The field inside the object is roughly $E \sim E_0/\epsilon_r$, and the current is $j = \sigma E$, which means that the heating is approximately

$$\dot{W} = \frac{j^2}{\sigma} \sim \frac{\sigma}{\epsilon_r^2} E_0^2 \tag{4.73}$$

This approximation is only valid as long as the skin depth, $\delta = \sqrt{2/(\omega\mu_0\sigma)}$, is large in comparison with the object size, i.e. $a \ll \delta$. In other cases, the problem becomes more complicated. In paper G we analyze the heating of a metal ball in a microwave field. The full solution for the electromagnetic problem is well known analytically, and typically refered to as the Mie solution [39, 40], but evaluating the heating term involves the calculation of some rather complicated series including Bessel functions of different kinds. Instead of devoting ourselves to this rather laborous calculation we used two asymptotic expressions for the heating, valid in the limits where $\delta \ll a \ll \lambda$,

and $\delta \ll \lambda \ll a$, corresponding to the quasistatic and geometrical optics domain respectively. It was found that both of the asymptotic expressions for the heating power scale as

$$\dot{W}_{\mathrm{Tot}} \propto \sqrt{\frac{\omega}{\sigma}} a^2 E_0^2 \tag{4.74}$$

Which means that the heating power increases slowly with respect to increasing frequency and decreasing conductivity, whereas it increases rapidly with increasing radius and applied field strength. Naively one would interpret this as if the equilibrium temperature reached by a large ball is higher than for a small ball. However, there are two very important effects which determine the equilibrium temperature. The mass of the ball (and the total thermal capacity) increases with the cube of the radius, which means that the time it takes to reach the equilibrium temperature rises rapidly with ball radius. Furthermore, the heat loss for small spheres scales linearly with radius. This means that for small balls, the heat loss rate for realistic field strengths becomes much higher than the heating rate. Consequently, there can exist an optimal range of ball radii, within which the heating of the ball is not negligible, and the temperature around the ball can rise significantly. This can lead to the existence of a third threshold, E_{III}, which is lower than the two defined in the previous paragraph. This threshold corresponds to an external field which is strong enough to heat the ball, and the surrounding air, to the point where the local breakdown threshold is lowered to the value of the local field. If the temperature at the surface of the ball is T_s, we can define this threshold by

$$T_s(E_{\mathrm{III}}) = T_b \tag{4.75}$$

$$T_b = T_0 \frac{E_{b,0}}{\gamma E_{\mathrm{III}}} \tag{4.76}$$

To find the surface temperature as a function of the heating power, it is necessary to solve the thermodynamical problem. The general equation for the temperature evolution reads

$$\rho c_p \frac{\partial T}{\partial t} = \nabla(\kappa \nabla T) + \dot{W} \tag{4.77}$$

In general, this equation can be very hard to solve, but for the case of a metal sphere in air, it is rather easy. Since the heat conductivity, κ, in metals is much higher than that of air, the temperature inside the ball can

be considered as homogeneous, and the equation can be integrated over the sphere volume to give

$$\frac{4\pi a^3}{3}\rho c_p \frac{\partial T_s}{\partial t} = -4\pi a^2 h_a (T_s - T_0) + \dot{W}_{\mathrm{Tot}} \tag{4.78}$$

where h_a is the average heat transfer coefficient, and W_{Tot} corresponds to the heating terms discussed above. For small spheres, heat is removed purely by conduction in the air, and the heat transfer coefficient can be approximated by $h_a \approx k_0/a$, where $k_0 \approx 0.025$ W m^{-1}K^{-1} [41] for air at room temperature. For larger spheres, convection becomes very important and the value of h_a has to be evaluated using empirical formulas and data from tables. The main conclusion of paper G is that the larger the sphere, the longer time it takes to reach the breakdown temperature, and the smaller the sphere, the larger are the heat losses, and the closer the third threshold is to the second threshold. Therefore, in experiments, it might be hard to distinguish any thermal effect on the breakdown threshold which is due to the absorption of microwaves by conducting objects. Either because the threshold is too close to the room temperature threshold, or that the time it takes to heat the object sufficiently might be longer than what the microwave generator can provide a continuous wave. This conclusion is valid for any shape of metal object that is thermally isolated from any conducting parts. If on the other hand, the absorbing object is in thermal contact with e.g. a waveguide wall, the heat loss is raised dramatically, and the thermal effect is reduced accordingly. This might explain why in all the openly published material, there are only two mentions of metal objects having a thermal effect on the breakdown problem. Acampora and Sprowl [42] studied the heating of microscopic copper spheres in a resonator ring filled with SF_6. They found that the heating can be quite large, but SF_6 has a breakdown strength which is four times higher than air, which means that the applied power without breakdown can be sixteen times higher than for air (see Eq. (4.74)), and the corresponding heating of the ball becomes 16 times higher. The second study was made by Beust and Ford [43]. They dropped metal fragments through waveguides filled with air, and noted that the fragments became glowing and hot while falling, and was able to induce thermal breakdown, whereas when the fragments where in contact with the waveguide walls, they never reached the required temperature. Finally, Nakamura et al. [44] found that trying to ignite a discharge using a stainless steel screw was ineffective, whereas a stick made of wood glowed red immediately upon insertion into the waveguide, and caused the formation of a breakdown plasma.

Chapter 5

Multipactor breakdown

5.1 Multipactor

Multipactor, or multipaction, is the exponential buildup of free electrons in a near vacuum, high power, high frequency device due to the multiplication of electrons by secondary emission from electron impacts on the device walls. It was first described by Farnsworth in 1934 [8], and suggested as a way of enhancing currents, in particular for the use in television. In the first half of the 20th century, this was the main application of multipactor [45]. With the advent of satellites and particle accelerators it was realized that multipactor might cause serious problem to the operation, and actually be the limiting factor for the power output of the device. The multipactor discharge will absorb microwave energy, create unwanted harmonics and noise, lead to heating of surfaces, possible outgassing and subsequent corona breakdown. The United States seemes to have taken this problem very seriously during the 60's and 70's, and consequently there is a large amount of both experimental and theoretical material available both in open journals, and nowadays in unclassified reports from NASA and similar entities. Naturally, the USSR also showed a great deal of interest in the multipactor phenomena, and the openly published material from the 60's and 70's is most likely just a fraction of the total research results. From the 90's and onwards, most research have been performed in Europe and Russia, by ESA, CNES, and associated entities and universities. There is a wealth of accessible research material, which continues to increase at a rapid pace. Despite over fifty years of research (or maybe because), there still seems to be some disagreement about a number of fundamental questions. The basic elements of the multipactor phenomena are easy to understand, and there is a consensus

about what they are. The multipactor phenomena is due to electrons causing secondary emission from impacts with surfaces. These surfaces can be conductive or dielectric, and the electron multiplication can take place on one surface or several. There are three necessary ingredients that have to be present for multipactor to develop. First, the system must be operating in vacuum or near vacuum conditions. Otherwise the electrons will suffer collisions with gas molecules, and although secondary emission can still occur at surfaces, the importance of this electron source diminishes rapidly with increasing pressure. The second ingredient is oscillating electric fields. For the secondary electrons to be able to gain energy, and escape the emission surface, the field has to change polarity sufficiently often. Third and finally, the surfaces must have a secondary emission yield maximum which is higher than unity.

Aside from these three necessary ingredients, there is no real consensus. For example, under what conditions is resonant electron motion important? Does the secondary emission curve approach unity for low electron energies, or does it go to zero? How does measured secondary emission curves relate to actual experiments on multipactor, and what is the distribution of electron emission velocities? These are just a few of the issues which are still unclear. Since there are different views on such fundamental issues, any presentation will have to be biased, otherwise, it will be overly lengthy and confusing. Having said this, we can proceed with the theoretical treatment. We will keep to electron motion in vacuum, and focus mainly on the parallel plates system, for it contains the basic components, but is relatively simple to analyze. Finally, we will discuss how to treat more complicated geometries without resorting to simulations, by using the ponderomotive force, and the geometrical spreading of electron bunches.

5.2 Electron motion and secondary emission

According to Eqs. (3.20), the electron motion in a homogeneous electric field in vacuum is described by

$$\begin{aligned} \bar{v}(t) &= \frac{e\bar{E}_0}{m\omega}\cos\omega t + \bar{v}_e - \frac{e\bar{E}_0}{m\omega}\cos\omega t_e \\ \bar{r}(t) &= \frac{e\bar{E}_0}{m\omega^2}\left[\sin\omega t - \sin\omega t_e\right] + \left[\bar{v}_e - \frac{e\bar{E}_0}{m\omega}\cos\omega t_e\right](t - t_e) \end{aligned} \tag{5.1}$$

where t_e is the time of emission. The magnitude of the oscillatory velocity, v_ω, is given by $v_\omega = eE_0/(m\omega) \propto E_0/\omega$. Since both the oscillatory velocity

and the drift velocity are proportional to E_0/ω, a breakdown threshold, E_b, for a specific frequency, ω, is easily converted to a different frequency, ω', through

$$E_b' \approx \frac{\omega'}{\omega} E_b \tag{5.2}$$

This is only a rough estimate, for other effects might be sensitive to the absolute value of the field and the frequency.

Secondary emission of electrons from a surface takes place because an impacting electron deposits its kinetic energy into the material. This energy is absorbed by electrons in the material, and given sufficient energy, one or more electrons can overcome the potential well of the surface, and be released as secondaries. Electrons are discrete particles, which means that given a particular impact energy, there is a certain probability that 0, 1, 2, 3 electrons or more will be released. When measuring the secondary emission yield of a certain material, the surface is bombarded with a huge number of monoenergetic electrons, and the secondary current is measured. What one measures is thus the average emission number for a certain electron energy, and by scanning the energy spectrum one ends up with a continuous curve of secondary emission yield (SEY) as a function of impact energy. There are two main features of this curve that everybody agrees upon. There is a first cross-over point, above which the SEY is higher than unity, and there is a second cross-over point, above which the SEY drops below unity. The first cross-over point has to do with the work function of the surface, and the fact that electrons in the surface need to receive enough energy to overcome it. The second point has to do with the depth at which the impacting electron releases most of its energy. If the velocity of the electron is too high, most of its energy will be released deep inside the material, and the probability of an electron reaching the surface and escaping becomes low. By tilting the impact angle of electrons away from perpendicular, more of the electron kinetic energy will be deposited in the near surface layer, and the SEY generally goes up. The standard way to model the SEY curve nowadays is called the Vaughan approximation, and was a curve fit introduced by Vaughan in 1989 [46]. The most simple version can be written

$$\sigma = \sigma_{\max} \left[\epsilon_i \exp(1 - \epsilon_i)\right]^{\beta} \tag{5.3}$$

where $\epsilon_i = v_i^2 / v_{\max}^2$, v_i is the electron impact velocity, $v_{\max}$ is the velocity corresponding to the maximum of the SEY curve, $\beta = 0.62$ for $\epsilon_i < 1$, and 0.25 for $\epsilon_i \geq 1$. The characteristic appearance of this curve is seen in Fig. 5.1.

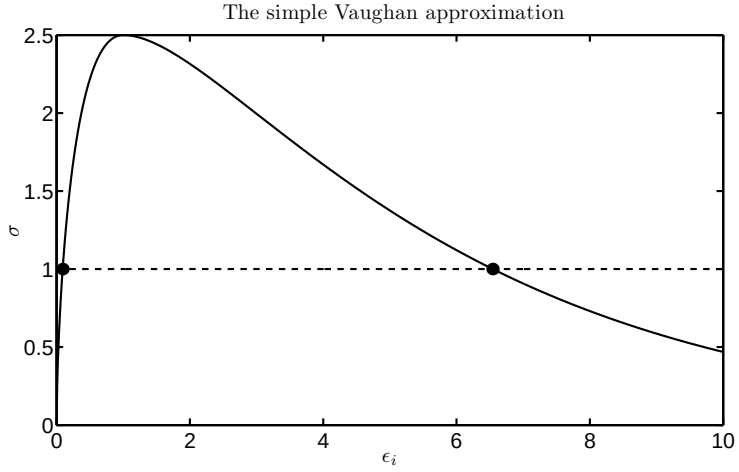

Figure 5.1: The appearance of the simple Vaughan approximation for the SEY. In this case, the maximum SEY is 2.5. The first and second cross-over points are marked with black dots, and below the dashed line, multipactor is impossible.

A necessary criterion for the existance of multipactor is thus that the maximum impact velocity (3.23), $v_{\max}$, is larger than the first cross-over velocity, v_1, i.e.

$$v_e + 2v_\omega > v_1 \tag{5.4}$$

The lower breakdown threshold is thus given tentatively by

$$E_b = \frac{m\omega}{2e}(v_1 - v_e) \tag{5.5}$$

It is more common to give the energy in eV corresponding to the emission and cross-over velocity

$$E_b = \omega\sqrt{\frac{m}{2e}}(\sqrt{W_1(eV)} - \sqrt{W_e(eV)}) \qquad \text{V cm}^{-1} \tag{5.6}$$

For the parallel plate system, the typical way of presenting the breakdown threshold is by plotting the voltage as a function of the gap-frequency product. If the gap has a width d, the voltage is $U_b = E_b d$, and the threshold is simply a linear function of the gap-frequency product

$$U_b = d\omega\sqrt{\frac{m}{2e}}(\sqrt{W_1(eV)} - \sqrt{W_e(eV)}) \qquad \text{V cm}^{-1} \tag{5.7}$$

We mentioned earlier that the frequency must be sufficiently high for a discharge to develop. For the parallel plates system, a rough value for this limiting frequency can be found quite easily. When the gap width is too small, the emission velocity alone will cause the electrons to traverse the gap in less than one half period. This makes resonant multipactor impossible, and occurs when

$$d\omega < \pi v_e \tag{5.8}$$

To construct a basic diagram of the multipactor threshold we also need an upper voltage. How to find it is not so obvious though. As the voltage is increased, electrons become more energetic, and at a certain voltage, the fastest electrons will have an impact energy above the second cross-over point, causing a net decrease in the number of electrons upon impact. The rate of the electron avalanche will then decrease, but it will not be supressed completely, for low energy impacts can still drive the avalanche. It is unclear at what voltage these low energy electrons will be unable to cause a multipactor discharge. In the case of resonant multipactor, the limit should be set by considering the finer details of resonance and phase stability, but in the non-resonant regime, the issue is still unresolved. We defer this question, and simply state that multipactor becomes suppressed when

$$2v_\omega + v_e \gg v_2 \quad \Leftrightarrow \quad U \gg dw\sqrt{\frac{m}{2e}}(\sqrt{W_2(eV)} - \sqrt{W_e(eV)}) \tag{5.9}$$

where v_2 corresponds to the second cross-over point.

An important effect both in resonant and non-resonant multipactor is the fact that electrons emitted at the wrong phase will impact the emission surface before making impact with the opposing surface. These electrons will contribute only slightly to the discharge, and it is important to divide the electron population into a "short range" and a "long range" phase interval. The short range electrons return to the surface quickly, whereas the long range electrons move away from the surface of emission, and will only return due to the work of some external agent, e.g. a ponderomotive force, a magnetic field, or a DC potential. Finding the short range boundaries consist in solving Eq. (3.20) for

$$\begin{aligned} &r(t_i) < 0 \\ &t_i - t_e \leq \frac{n\pi}{\omega} \end{aligned} \tag{5.10}$$

Actually, there are only two cases: when $n = 1$, and when $n \geq 2$, corresponding to impact on the emission surface within one half period, and one period respectively. If an electron does not impact the emission surface within one complete period, it will not do so at all, unless forced so by some external agent. The solution to (5.10) for $v_e > 0$ has to be found numerically, and the appearance of the solution for $n = 2$ can be seen in Fig. 5.2.

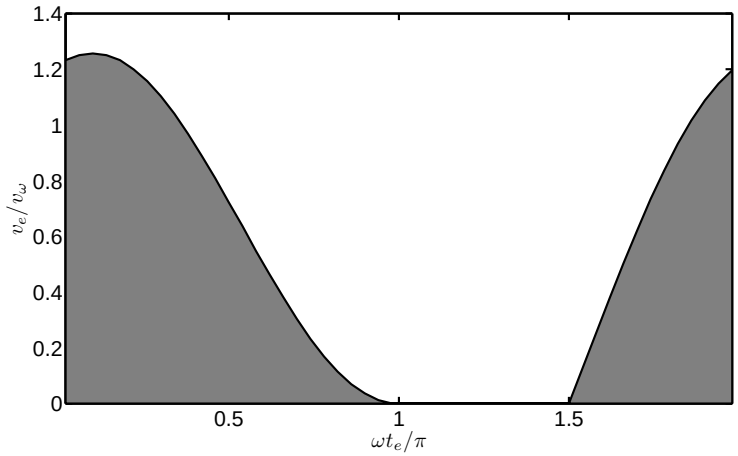

Figure 5.2: The limits for short range emission for orders of multipactor above one. Grey areas are short range, white long range.

5.3 Resonance theory

From the earliest theoretical ventures into the field of multipactor [47–51], the resonance theory has been completely dominant, even though the agreement with experiments has been rather limited. The fundamental assumption is that the influence of any spread in electron emission velocity has a negligable effect on the discharge dynamics. This is true when the drift motion caused by the emission velocity spread, Δv_e is much smaller than the distance an electron covers in a period, i.e.

$$\Delta v_e \ll \frac{2\pi}{\omega d}(v_e + v_1)^2 \tag{5.11}$$

where we have assumed that the gap is traversed in a time $d/(v_e + v_\omega)$, that $\bar{v}_e$ is entirely in the direction of the surface normal, and $v_\omega \geq v_1$. When this assumption holds, the electrons have to impact at a certain instant

depending on its emission time. For the parallel plate system, an electron must impact the opposite plate when the field is reversed in comparison with the field at the emission instant. This means that the impact time, t_i, is related to the emission time by

$$t_i = t_e + n\frac{\pi}{\omega}, \quad \text{where} \quad n = 1, 3, 5, 7... \tag{5.12}$$

If an electron starts at $r(t_e) = 0$, it must impact at $r(t_i) = d$, and using Eq. (3.20) we find

$$v_{\omega,r} = \frac{v_e n\pi - d\omega}{2\sin\omega t_e + n\pi\cos\omega t_e} \tag{5.13}$$

For this electron to make a contribution to the avalanche, the impact velocity must be above v_1 and below v_2. Using Eq. (3.20) we get

$$v_1 < v_e - 2v_{\omega,r}\cos\omega t_e < v_2 \tag{5.14}$$

From Eqs. (5.13) and (5.14), the resonant limits can be found by solving

$$\tan(\omega t_e) = \frac{1}{2}\left[\frac{2d\omega - n\pi(v_e + v_{1,2})}{v_{1,2} - v_e}\right] \tag{5.15}$$

The resonance limits do not take into account the fact that an electron might strike the plate from which it was emitted before it makes impact with the second plate. To see when this happens, it is necessary to solve

$$r(v_{\omega,r}, t_e + \Delta t) < 0, \quad \text{where} \quad \Delta t < n\pi/\omega \tag{5.16}$$

Solving the equation above is not too difficult using a computer, and the solution for $n \geq 2$ is shown in Fig. 5.2. Taking consideration of these short range electrons will augment the resonance zones, and make them smaller. What is even more restrictive for the size of the resonance zones is the condition of phase stability. The emission phase of an electron can be disturbed by fluctuations in emission time delay, emission velocity, field strength etc., and for the discharge to be able to develop, the electrons should be emitted in a phase region where the delay in the impact phase becomes smaller than the emission time delay. The condition for phase stability can be found by perturbing Eq. (3.20) with the phase delay δt_e, and expressing the impact time delay δt_i as a function of this pertubation.

$$G = \left|\frac{\delta t_i}{\delta t_e}\right| = \left|\frac{v_e - v_\omega n\pi\sin\omega t_e}{v_e - 2v_\omega\cos\omega t_e}\right| \tag{5.17}$$

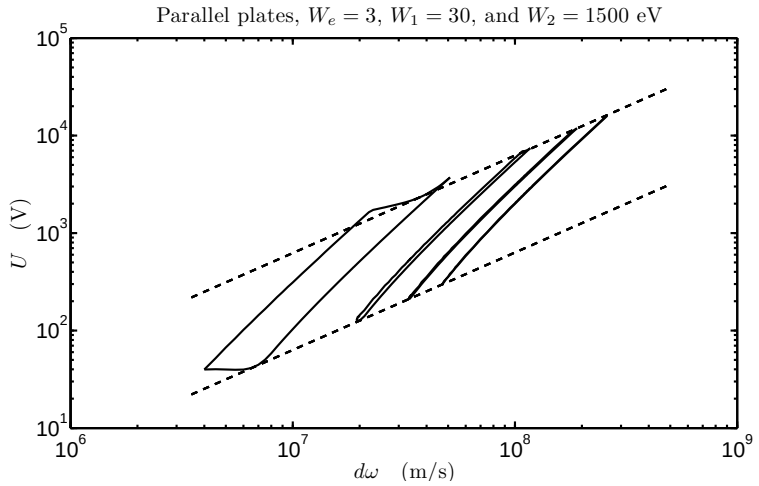

Figure 5.3: The first four susceptibility zones for a material having $W_e = 3$, $W_1 = 30$, and $W_2 = 1500$ eV. Dashed lines represent the approximations given by Eqs. (5.5) and (5.9), and they are drawn starting from the left limit given by Eq. (5.8).

The phase is considered as stable when $G < 1$. In Fig. 5.3 the typical appearance of the first few susceptibility zones is shown along with the approximations Eqs. (5.5), (5.8) and (5.9).

In a resonant discharge, electrons from a very limited phase range are involved. In a region of unstable phase, the electron bunch will dilute upon transits, and if this dilution is strong enough, an electron avalanche cannot develop. But the condition that G must be smaller than unity is actually a bit restrictive, for the SEY of the impacting electron bunch might be high enough to counteract the electron dilution. Taking account of this will broaden the susceptibility zones, but to what extent depends on the maximum SEY. We shall not investigate this issue further, but rather sum up the important features of resonant multipactor. The electrons involved in an avalanche must cross the gap in the time $n\pi/\omega$, the impact velocity must be between the two cross-over velocities, and the emission and impact must be in a phase range which is sufficiently stable not to dilute the electron density at a faster rate than the SEY at this particular impact speed will make it grow.

Naturally, taking account of these criterias for geometries more complicated than parallel plates is hard, and in general impossible. Despite this, some geometries have been investigated quite thoroughly using approximate methods, for example circular [52], rectangular [53, 54], coaxial [55–58] and

wedge-shaped waveguides [59,60], as well as the waveguide iris [61]. In addition to this, analysis have been performed on mixed and modulate microwave signals [62–64], and in low pressure gas [11].

5.4 Statistical theory

When the transit time of electrons becomes long, i.e. for higher order multipactor, the emission velocity spread will gradually destroy the resonance. This happens at

$$\Delta v_e \sim \frac{2\pi}{\omega d}(v_e + v_1)^2 \tag{5.18}$$

When the resonance starts to be destroyed, an electron bunch emitted at a specific time will impact over a certain interval. The size of the interval depends on the spread in the emission velocity coupled with the transit time. If the gap width becomes very large, the electron bunch will spread out so much that it will cause impacts during several periods. In this case we have entered the non-resonant regime, and it is possible to use the simplified impact statistics decribed later in section 5.5.

Obviously, in this regime, the condition of phase-stability becomes very problematic, and in order to treat the intermediate region properly one needs to consider the probability of an electron being emitted at a specific time hitting the critical surface at a specified time. Such an analysis relies on a detailed knowledge of the electric field configuration as well as the emission velocity distribution. A sophisticated mathematical framework to perform this type of analysis has recently been developed and applied to some different situations [65–71]. The model keeps track of the evolution of a population of electrons using transit probability functions. The proceedure is rather involved and can only be performed using numerical routines for systems where the probability functions can be found explicitly. This limits the application of the method to basically the same systems as those which can be analyzed using the resonant framework.

The major effects of resonance being destroyed are that the phase range of electrons participating in the discharge will become wider, and the threshold goes up. The rise in the threshold is due to two effects. Since electrons will be less tied to the resonant condition, the mean impact speed will tend to decrease, and for systems operating close to the lower threshold, this means a reduction in the effective SEY. The spread in impact time will also lead to an increased loss of electrons into regions where the SEY is low or the secondaries will be short range. This effect is equivalent to the phase

defocusing in the previous section. The lower envelope of the susceptibility chart will be raised, due to the higher electron losses, but the resonance zones will start to blur into each other, and multipactor will become possible in regions where the resonance theory says it shouldn't be. For sufficiently long transit times, resonance is destroyed completely, and the multipactor zones blur into a continuum. In this region it is possible to use a more simplified treatment, which is discussed in the next section.

5.5 Non-resonant theory

When transit times become long enough, the discharge can be described using a simplified version of the statistical theory, typically called the non-resonant or polyphase approach. The fundamental assumption is that electrons will be evenly distributed in space. The reason for this is simple. Consider an electron bunch being emitted at a specific phase. The electrons will drift away from the emission surface, at first being collected in a very thin sheath. Such sheaths emitted during consecutive periods will be separated in space by a distance $2\pi(v_e + v_\omega)/\omega$, but as they drift towards the other surface the emission velocity spread will cause these sheaths to become wider. In the limit when

$$\Delta v_e \gg \frac{2\pi}{\omega d}(v_e + v_1)^2 \tag{5.19}$$

electrons emitted from different periods will overlap in space, forming a continuous sheath moving towards the other surface. This allows one to use a much simpler statistical treatment than those described in section 5.4. This statistical method was developed and applied during the 70's by a group in Moscow [72–78], who found all of the key results, but the full application of the model was not possible at that time, due to the limited available computer capacity. Nowadays, this is not an issue, and all the complexities can be taken account of in codes which takes only a few seconds to execute.

In the non-resonant approach one considers a distribution of electrons with different emission phases, forming a continuous sheath, which moves towards a surface. Since electrons will hit the surface at a higher rate when the electrons are moving rapidly, the smooth distribution in space will not give rise to a smooth impact distribution. Electrons that have a large drift velocity, $v_d \geq v_\omega$, i.e. emitted close to $\omega t_e = \pi$, will form an impact distribution described by

$$n_i(t_i) = N\frac{\omega}{2\pi v_d}(v_d - v_\omega \cos\omega t_i) \tag{5.20}$$

where N is the total number of electrons that will impact during one field period.

If one recalls the limits for long range emission displayed in Fig. 5.2, one quickly realizes that a large portion of the impacting electrons will only give rise to short range emission. If the emission speed is negligable, the long range emission interval goes between $t_i = \pi/\omega$ and $3\pi/(2\omega)$. The number of impacts in this interval is

$$\int_{\pi/\omega}^{3\pi/(2\omega)} n_i(t_i)dt_i = \frac{N}{4}(1 + \frac{2}{\pi}\frac{v_\omega}{v_d}) \tag{5.21}$$

If $v_d = v_\omega$, the fraction of impacts in the long range interval becomes $(1 + 2/\pi)/4 \approx 0.41$. Since short range emission contributes only slightly to the total number of secondaries, for low emission energy, there will be an effective loss of electrons at around 60 %, which has to be balanced by high values for the secondary emission in the long range emission interval. This is the most important consequence of the non-resonant approach. Fast electrons will impact over the entire field period, whereas electrons with a low drift velocity will tend to strike mainly in the long range interval. Furthermore, in a non-resonant double-sided discharge, all electrons with a positive drift velocity will take part in the impact emission process. This means that one has to consider the impact statistics of a distribution of electrons over drift speed, or eqiuvalently, emission phase. This leads to an average impact speed which is substantially lower than the maximum value $v_{d,\max} + v_\omega$. This is the second major consequence of entering the non-resonant regime, and the necessary voltage for breakdown becomes higher in comparison to the resonant case. In the non-resonant regime, emission time is only linked to impact time through the drift energy of the electron, which dictates the phase region where impact is possible, and determines the probability for impact at a certain point in this interval. Obviously, this also means that the criterion of phase stability looses all relevance.

To be able to describe the impact statistics of a distribution of electrons over emission phase one needs to introduce a distribution function $\eta_i(t_i, t_e)$, which describes the fraction of impacts at a certain instant, t_i, from electrons with a certain emission phase, t_e. The number of impacts, $n_i(t_i)$, at a certain time, t_i, is thus

$$n_i(t_i)dt_i = \int_{t_{e,\min}}^{t_{e,\max}} \eta_i(t_i, t_e)dt_i dt_e \tag{5.22}$$

The impact distribution has to be connected with an incoming electron distribution, $n(t_e)$. The incoming electrons are evenly distributed above the surface in a height interval which depends on the drift speed for that particular emission time, t_e. So if there are $n(t_e)dt_e$ electrons in the incoming distribution which have an emission time t_e, these are evenly distributed over a height interval $2\pi(v_e - v_\omega \cos\omega t_e)/\omega$. The full connection between the incoming electrons and the impact distribution is rigorously derived in paper F, and found to be

$$\eta_i(t_i, t_e)dt_i dt_e = \frac{n(t_e)\omega}{2\pi} \frac{v_e - v_\omega \cos\omega t_e - v_\omega \cos\omega t_i}{v_e - v_\omega \cos\omega t_e} dt_i dt_e \tag{5.23}$$

This formulation assumes that the incoming electrons are generated at a surface with the same electric field strength, otherwise the emission speed has to be adjusted. In paper F we investigate the case of non-resonant multipactor between two parallel plates. This model is equivalent to single-sided multipactor in a coaxial or circular waveguide, where the emitted electrons are reflected by the ponderomotive force, and eventually returns to the surface of emission with their drift speed reversed. In the three cases mentioned above, secondary emission is described by a distribution over emission phase, $n'(t_e)$

$$n'(t'_e)dt'_e = \int_{t_{e,\min}}^{t_{e,\max}} \sigma(t'_e, t_e) \frac{n(t_e)\omega}{2\pi} \frac{v_e - v_\omega \cos\omega t_e - v_\omega \cos\omega t'_e}{v_e - v_\omega \cos\omega t_e} dt'_e dt_e \tag{5.24}$$

and at the breakdown threshold, the emitted distribution must match the incoming, i.e. $n'(t_e) = n(t_e)$. In general, the distribution which satisfies these equations can only be found numerically. This is mainly due to the complicated form of the SEY function, but also to the nontrivial evaluation of the minimum and maximum emission times ($t_{e,\min}$ and $t_{e,\max}$) which are able to cause impact at a certain instant t_i.

In paper F we find the steady state solution for a range of different parameter combinations. Furthermore, we also include the short range electrons into the calculations. In all the previous publications considering the non-resonant model, the short range electrons were ignored. The reason for this is most likely the limited computer capacity available at the time of

these studies. It is found that the influence of the short range electrons is indeed small but not at all insignificant.

The numerical evaluation of the electron distribution is very fast for the simple parallel plate system, and it is possible to draw general breakdown curves based on the simple Vaughan approximation for the SEY function. These curves can be found in paper F. In systems with a more complicated geometry, one has to identify the surfaces which are most vulnerable to double or single-sided multipactor. Then it should be possible to apply the concepts described in section 5.6 to evaluate the electron density and drift speed at different locations in the system. The exact proceedure for this is not yet clear, but there is no particular reason for why it should not be possible. Normally when one wants to consider multipactor in a complicated system, it is necessary to simulate the electron trajectories using the particle in cell or Monte Carlo methods. Unfortunately, such simulations tend to be very slow, due to the large number of trajectories one has to consider. Furthermore, it is often necessary to run many simulations, for the electron emission velocity and direction should follow some random distribution. This means that simulation results will suffer from random fluctuations. This is realistic, but it might lead to erroneous breakdown threshold values if the number of simulations is not large enough. Therefore it seems that the non-resonant model may be of great use for making fast, approximate assessments of the multipactor threshold in realistic systems.

5.6 Effects of inhomogeneities

So far we have only considered the parallel plate system, where the field is homogeneous and the surfaces are flat. Naturally, when the field and surface structure becomes complicated, electron trajectories can take on almost any shape. To study such trajectories it is often necessary to simulate them, but for systems where transit times are rather long and the surfaces can be considered as smooth, it is possible to describe the average electron motion using the concept of the ponderomotive force, and geometrical spreading. By using these concepts it is possible to evaluate the drift speed of electrons directly from the knowledge of the electric field strength, and the density of electron bunches from what is really the method of geometrical optics.

5.6.1 The ponderomotive force

If a charged particle is oscillating in a field with a moderate gradient, it will experience a force which tends to push the particle into regions of less intense

field. This non-linear force is called the ponderomotive or Miller force [79]. We will not perform the derivation of the force here, since it can be found in many textbooks [80, 81]. Suffice to say, depending on the circumstances, the force is caused by the action of the magnetic field ($\bar{v} \times \bar{B}$), the gradient of the electric field in the direction of motion, or the combination of both. It is actually remarkable that the force of the magnetic field and electric field can be combined in this very simple formula

$$\bar{F}_{\text{pond}} = -\frac{e^2}{4m\omega^2}\nabla E^2 \tag{5.25}$$

This equation is valid when the field gradients are not too large in comparison with the oscillatory motion of the electron, i.e. $e/(m\omega^2)|\nabla E| \gg 1$. Evidently, the force at any point is given by the local gradient in the electric field. This means that we can calculate the work , ΔW, done by this force in moving the electron between two points, $\bar{r}_1$ and $\bar{r}_2$, with the corresponding field strengths E_1 and E_2, as

$$\Delta W = \int_{\bar{r}_1}^{\bar{r}_2} \bar{F}_{\text{pond}} \cdot d\bar{r} = -\frac{e^2}{4m\omega^2}(E_2^2 - E_1^2) \tag{5.26}$$

Which can be rewritten as

$$\Delta W = \frac{m}{4}(v_\omega^2(\bar{r}_1) - v_\omega^2(\bar{r}_2)) \equiv \frac{m}{4}(v_{\omega,1}^2 - v_{\omega,2}^2) \tag{5.27}$$

This result is very useful, for the work done by the ponderomotive force affects the drift speed of electrons. Hence, in moving the electron from $\bar{r}_1$ to $\bar{r}_2$ the drift energy is changed an amount ΔW, and we get

$$\frac{1}{2}mv_{d,2}^2 = \frac{1}{2}mv_{d,1}^2 + \Delta W \quad \Leftrightarrow \quad v_{d,2}^2 = v_{d,1}^2 + \frac{1}{2}(v_{\omega,1}^2 - v_{\omega,2}^2) \tag{5.28}$$

If we consider an electron emitted from a surface at $\bar{r}_1$ we can see the fascinating consequences of this formula. The maximum drift velocity which the electron can attain is $v_{\omega,1}$, and we get

$$v_{d,2}^2 = \frac{3}{2}v_{\omega,1}^2 - \frac{1}{2}v_{\omega,2}^2 \Leftrightarrow v_{d,2}^2 = \frac{3}{2}\frac{e^2}{m^2\omega^2}E_1^2(1 - \frac{1}{3}(\frac{E_2}{E_1})^2) \tag{5.29}$$

Clearly, the drift velocity becomes zero when $E_2 = \sqrt{3}E_1 \approx 1.73E_1$. This means that, under the conditions when the ponderomotive force concept is valid, multipaction between surfaces with substantial differences in the field

strength is impossible. In paper C we analyzed the situation of multipactor between two parallel metal cylinders. In this case, doublesided multipactor becomes impossible when the cylinders differ too much in their respective radii. A similar situation is encountered in a coaxial waveguide when the inner conductor becomes too thin [55]. In this case however, single sided multipactor should be much easier to achieve than for the parallel cylinders case, simply due to the fact that in the first case, electrons cannot escape the systems, whereas in the second case, escape should be almost inevitable.

Using the above formulas, the drift velocity of an electron can be specified everywhere in the system, depending only on the relative positions, and not on the actual trajectory. This allows one to easily assess the risk of multipactor between different surfaces.

5.6.2 Geometrical spreading

Another concept, along with the ponderomotive force, which can be used to approximate the electron motion is that of geometrical spreading of electrons. For metals, the electric conductivity is very high, and the field is always normal to the surface. Since the main motion of secondary electrons is due to the initial acceleration of the field close to the surface, the emitted electrons will project outwards from the surface following the curvature of the surface. This is very much like light being emitted from a light bulb, where the intensity of the light decreases with the square of the distance from the bulb. In the same way, the density of electrons emitted from a sphere would decrease as the square of the distance. This geometrical effect does not necessarily have to result in a dilution of the electron density. A concave surface results in focusing of the electron density, but past the focal point, the density is decreasing again. For a depiction of this effect see Figs. 5.4 and 5.5.

The concept of geometrical spreading (or focusing) is very powerful, and it can be used in the intermediate range when the oscillation amplitude of an electron is much larger than the scale length for the fine-structure of the emission surface, and much smaller than the scale length for the electric field gradient.

In paper C and E, this geometrical spreading was used to model the dilution of the electron bunches during successive impacts on the parallel cylinders. Depending on the maximum SEY, there was a critical radius versus gap width, below which the diluting effect became greater then the maximum electron gain due to secondary emission, thus making multipactor impossible. Exactly how to express the spreading mathematically depends

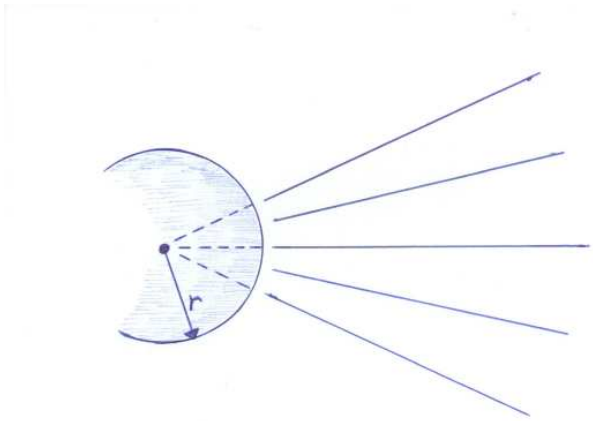

Figure 5.4: Geometrical spreading from a convex surface having the radius of curvature r. The focal point is inside the curved object.

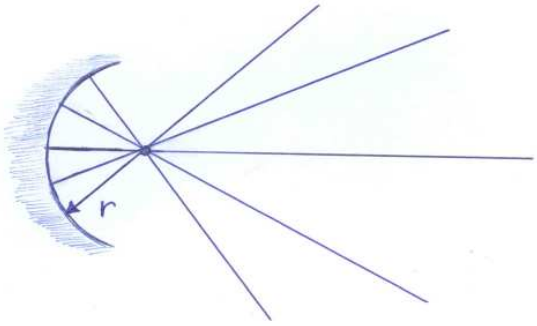

Figure 5.5: Geometrical focusing from a concave surface having the radius of curvature r. The focal point is outside the curved object, and within the distance to the focal point, the electron density increases as they move away from the surface. After passing the focal point, electron dilution from geometrical spreading starts.

on the geometry. In the case of parallel cylinders with radii r_a and r_b, the density, n_a, of a bunch of electrons possessing identical velocity starting at the surface of cylinder a and arriving at cylinder b is described by

$$n_b = \frac{n_a}{1 + d/r_a} \tag{5.30}$$

Upon impact with surface b, there will be emission of $\sigma_b n_b$ electrons. Consequently, the electron density which returns to surface a is

$$n'_a = \sigma_b \frac{n_a}{(1 + d/r_a)(1 + d/r_b)} \tag{5.31}$$

When these electrons impact surface a they will cause the emission of $\sigma_a n'_a$ electrons. Thus, for the electron density to grow while making successive impacts on the two surfaces, the following inequality must be fullfilled

$$1 < \frac{\sigma_a \sigma_b}{(1 + d/r_a)(1 + d/r_b)} \tag{5.32}$$

For cylinders of the same material and equal radii the condition becomes

$$1 + \frac{d}{r} < \sigma \tag{5.33}$$

Silver for example has a maximum SEY of 2.22 [82], which means that double-sided multipactor becomes impossible when $d/4 < r$. This is quite restrictive, and in practical systems, the radii might be much smaller.

Chapter 6

Summary and conclusions

The main aim of this thesis has been to explore different aspects of the breakdown problem which are outside the scope of the classical diffusion theory for the microwave corona breakdown, and the traditional resonance theory for the multipactor phenomena.

Regarding corona breakdown, it was clearly seen in papers A and B that at high gas pressures, when the attachment length is small with respect to the system dimensions, the breakdown plasma will be localized to the high field regions. This has long been recognized in the research community, but little has been done to investigate the further evolution of such breakdown regions. In paper D we analyzed the thermal stability of a spherical region of breakdown plasma in a homogeneous microwave electric field in air. It was found that there is a critical radius, which depends on the system parameters, under which the microwave energy which is absorbed by the ball is less than the heat which is transported over the ball perimeter, causing the ball to shrink and dissappear. Above the critical radius, the ball will absorb more heat than what is removed over the ball edge. This will cause the surrounding air to heat up, lower the breakdown threshold in the surrounding air, and lead to the expansion of the ball. The practical usefulness of this result is that is gives an order of magnitude estimate of the size of critical regions inside microwave systems. With critical regions we mean: the immediate vicinity of a field enhancement, caused e.g. by some irregularity in a conducting surface; and regions of local heating. The reason for a particular spot to become heated in a microwave system could in theory be the absorption of microwave energy by protruding conducting parts. In this case, there exist the possibility of three distinct breakdown thresholds. The first and highest one corresponding to breakdown in the unperturbed field;

the second intermediate one to breakdown in the enhanced field around the conductor protrusion; and the third and lowest one to breakdown caused by heating of the protrusion, the heating of the surrounding gas, and the subsequent lowering of the breakdown threshold in the surrounding gas. In paper G , we try to isolate the most relevant physical processes in this scenario by analyzing the heating properties of a metal ball subject to a homogeneous microwave field, and the effects on the breakdown threshold. This system has the benefit of having a low field enhancement, which allows the applied field, and the absorbed power, to be high without reaching the second threshold. Furthermore, since we assume that the ball is floating freely in air, the heat loss is minimized, meaning that the effect on the breakdown threshold is maximized. It was found that for small and large ball radii, the heating effects on the threshold are small, but in the intermediate region, it can be substantial, provided that the metal has a low conductivity, and the field frequency is high. This was a worst case scenario analysis. In realistic systems, protruding metal parts will always be in thermal contact with surrounding structures. Depending on the nature of the contact, the heat loss may increase dramatically, which leads to much less pronounced effects of heating on the threshold.

Although the studies in paper D and G can be used to formulate practical guidelines for certain systems, the main purpose was to highlight and clarify the relevant physical mechanisms, which can be somewhat hard to discern while perusing general textbooks and reports.

Regarding the multipactor phenomena, the main focus of our research has been to look at certain aspects of a quadri-filar helix antenna system. For low pitch angles, the conducting wires can be approximated by four parallel cylinders, and since the field will at all times be directed between two opposing pairs of conductors, we started our analysis in papers C and E by looking at two parallel infinite cylinders. The fact that a realistic antenna has a rather large conductor separation meant that we could simplify the treatment of the electron ballistics considerably. Under these circumstances, the electrons receive a drift velocity in the direction of the surface normal at the time of emission, and then drift outwards from the surface of emission while performing an oscillatory motion. The oscillations in the inhomogeneous field leads to an effective force directed out of high field regions, called the ponderomotive or Miller force. This force affects the drift velocity of the electrons, and since the field in the parallel cylinders system is known exactly, this allowed us to specify the drift and oscillatory velocity at each point in the system relative to another. Using an average value for the electron impact velocity, based on the non-resonant assumption, we

could evaluate the risk of multipactor depending on the system dimensions and surface characteristics. In the case of cylinders of unequal radii, the ponderomotive force will cause electrons emitted from the larger cylinder to slow down before reaching the smaller cylinder. When the radii become to dissimilar, two-sided multipactor becomes impossible.

An even more important and interesting effect is the dilution of the electron density during successive gap passages. This is due to the fact that the local field is always normal to the surfaces, and that the emission surfaces are convex. In fact, when the radius of curvature becomes much smaller than the gap width, the electron dilution becomes so strong that multipactor for realistic values of the maximum secondary emission yield becomes impossible.

To corroborate the theoretical findings in paper C, a set of simulations was performed using a Monte Carlo code. The marked dependance of the breakdown voltage on the cylinder radii as compared to the gap width was found to be very similar in the calculated and simulated results. But the value of the breakdown threshold was significantly higher in the simulations. There might be several reasons for this. In the calculations, it was assumed that only the most energetic electrons took part in the discharge, and that the emission velocity could be neglected. In the simulations however, it was necessary to include a finite emission velocity, and to provide a stochastical element. In this case the angle of the emission velocity with respect to the surface normal was randomized. This means that electrons from different emission phases will be involved in the discharge, and that the discharge was non-resonant in nature. To explore more exactly the effect of non-resonance, a detailed study of the emission and impact statistics was undertaken in paper F. Besides rederiving and presenting the theoretical framework, two important effects were highlighted. Since electrons from a band of emission phases are involved in a non-resonant discharge, it will lead to a lower average impact velocity, which raises the breakdown threshold. But even more importantly, the spread of electron impacts over the entire field period leads to a significant number of impacts in regions where the secondary electrons are effectively lost due to immediate reabsorption. Under certain circumstances this effect will remove half of the impacting electrons, and constitute an important electron loss source indeed. Since the non-resonant regime is hard to explore in simulations, the statistical treatment offers an alternative way of analyzing complex systems. If one combines the geometrical spreading effect, the ponderomotive concept, and the non-resonant statistical treatment, it should in principle be possible to quickly assess the risk of multipactor in systems that are to complicated to

yield to direct analysis and simulations.

Chapter 7

Summary of included papers

Paper A

In this paper we determine the microwave breakdown threshold for air in a rectangular resonator cavity. We use the diffusion theory described in section 4.2 to find the critical value of the electric field which is able to cause breakdown as a function of the effective pressure, field frequency, and the cavity dimensions. The eigenvalue problem is solved through approximate variational techniques, and numerical relaxation methods. Aside from presenting the breakdown threshold curves, the main conclusion is that the discharge becomes localized to the center of the cavity for high pressures, corresponding to the attachment controlled breakdown described in sections 4.3.1 and 4.3.2.

Paper B

In this paper we use the same equations and methods as in paper A to study the breakdown characteristics of three different geometries: a step-like ionization profile (the same which is analyzed in section 4.3.2, an exponential ionization profile, and the case of a small hemispherical conductive boss on an infinite conductive plane. The results in the paper clearly demonstrates how the sensitivity of the breakdown threshold depends on the size of the field inhomogeneity and the pressure. In the diffusion dominated regime, small inhomogeneities have no influence on the threshold and breakdown takes place in the entire volume, whereas in the attachment dominated regime, the breakdown threshold is set by the field inside the inhomogeneity, and the corresponding region of breakdown plasma can be very small. It

is clearly pointed out that the damaging effects of such a small breakdown region are not obvious, and warrants further investigation. This conclusion provided strong motivation for the investigations performed in papers D and G.

Paper C

In this paper we determine the criterias for multipactor in a system consisting of two parallel infinite conductive cylinders. The motivation for this study was the need to develop practical guidelines for a quadri-filar helix antenna used for satellite communications. Due to the complexity of this antenna, the parallel cylinder geometry was chosen as a first approximation, allowing us to highlight the most relevant physical effects, namely: curved surfaces, an inhomogeneous field profile, and an open geometry. The exact electron trajectories in such a system are not trivial, but since realistic antennas have a rather large gap width, the electrons could be assumed to be non-resonant, moving according to the geometrical theory which was explained in section 5.6.2, while being affected by the ponderomotive force described in section 5.6.1. It was found that the geometrical spreading effect for large gap to radii ratio gives rise to very high electron losses, which renders double-sided multipactor impossible.

Paper D

In this paper we investigate the thermal stability properties of a small spherical breakdown region in air. The motivation for this study came mainly from paper B, where the question was asked: does a small breakdown region have to be dangerous for the operation of a microwave device? Since plasma forming in a microwave field will perturb the field, and absorb radiation, the problem of finding self-consistent solutions for both the field and shape of the plasma as a function of time is formidable indeed, see section 4.4.1. In fact, to treat the more general problem, it is questionable if exact solutions should be sought in the first place; since the form of the plasma will be so heavily dependant on the field structure, and surrounding geometry. To limit the complexity of the problem, and isolate the main effects, we studied a plasma with a given form, that of a spherical patch inside a field which is homogeneous, and below the breakdown threshold. The plasma is assumed to have been generated by some rapid heating source which is then immediately switched off. The radiation which is absorbed by the plasma heats the

gas, lowers the effective pressure, and maintains the partially ionized state. At the same time, the field inside the sphere is reduced to the breakdown threshold by the net dipole moment of the electrons oscillating in the field. Given these prerequisites, the remaining problem is of a thermodynamical nature. If the ball absorbs more heat than what it looses over the edges, the plasma may expand into the surrounding air, whereas if it looses more heat than what is generated, it will shrink. There is in fact a critical radius of the original spherical plasma region, above which the plasma will expand, whereas below it, the plasma will shrink. We find an expression for this radius as a function of the field strength and wavelength, and the thermodynamic parameters for air.

Paper E

In order to validate the theoretical results from paper C, simulations of the parallel cylinders system were performed, using a Monte Carlo software, for two different gap widths, and a range of different radii. The characteristic shape of the curves describing breakdown voltage as a function of radii were clearly replicated by the simulations, but the exact value of the breakdown voltage was found to be markedly higher in the simulations as compared to the approximate theory. The reason for this appears to be the effects of non-resonance, which is the subject of paper F.

Paper F

In the case when electron transit times are long, the multipactor discharge can be described using the non-resonant approach, which is briefly described in section 5.5. The fundamental assumption is that electrons arriving to a surface can be assumed to be evenly distributed in space. The reason being the effect of a thermal spread in electron emission velocity. To treat the multiplication of electrons due to secondary emission in this case one needs to apply statistical methods. In this paper we rederive the mathematical framework needed to treat the discharge, and apply it to the case of breakdown between similar surfaces in a homogeneous field. This makes the results immediately applicable to three system, single-sided multipactor in coaxial and circular waveguides, as well as double-sided multipactor in a parallel plate system. The main result of this study is that the breakdown threshold is significantly raised in comparison with the resonant case. This is due to two effects. First, since the electrons will impact during a certain

phase interval depending on their drift velocity, the average impact velocity goes down, which raises the necessary field for breakdown. Second, the spreading of the impact phase means that a significant number of electrons will impact during phases which cause very little secondary emission. This is the most important effect, and can lead to significant electron losses for small relative values of the electron emission velocity. In order to validate the concepts and quantitative predictions made by the theory, a Monte Carlo software was created to simulate the simple case of multipactor between two parallel plates. It was found that when the plate separation becomes large, the non-resonant theory seems to predict accurate values for the breakdown threshold, and the impact statistics appear to be analogous.

Paper G

In this paper we analyze the heating of a metal ball irradiated by a homogeneous electromagnetic wave, and the subsequent effect on the breakdown threshold in air. The motivation for the study was the unresolved question about the heating of conducting elements inside microwave systems, and the risk for thermally induced breakdown. Since the solution for the electromagnetic field given by the Mie theory is rather complicated, two asymptotic forms for the ball heating, valid for small balls, and large balls respecttively, were used to approximate the more complicated heating function. To treat the heat loss from the ball, empirical expressions were used taking into account both conduction and convection, but neglecting radiation. Since the heating depends heavily on the electrical conductivity of the metal, and the field frequency, four different limiting cases were analyzed in greater detail. On the low end of the scale with regards to conductivity, the stainless steel type A2 was used, whereas for high conductivities, silver was chosen as a good representative. The problem was solved for 1 GHz, and 100 GHz, corresponding to the upper and lower parts of the microwave spectrum. The general conclusions were that in any system with metal objects that enhance the field and absorb microwave energy, there is the possibility of three distinct thresholds. The first, and highest, represents breakdown in the unperturbed field. The second, breakdown in the region of enhanced field. And the third, lowest, breakdown in the enhanced field due to gas heating. More specifically, it was found that there exists a range of ball radii, depending on the material, where the heating of the ball is the most effective, and the effects on the breakdown threshold might be large, whereas outside this range, heating is negligable, and the effects on the breakdown

threshold very small.

References

[1] A. Anders, "Tracking Down the Origin of Arc Plasma Science I. Early Pulsed and Oscillating Discharges", *IEEE Trans. Plasma Sci.*, **31**, 4, 1052 (2003).

[2] J. S. Townsend, *The Theory of Ionization of Gases by Collision*, Constable & Company LTD, London (1910).

[3] L. B. Loeb, *Basic Processes of Gaseous Electronics*, University of California Press, Los Angeles (1955).

[4] W. O. Price, *Corona Onset in Flight*, Doctoral Thesis, Griffith University, Australia (2009).

[5] M. A. Herlin, and S. C. Brown, "Breakdown of a Gas at Microwave Frequencies", *Physical Review*, **74**, 3, 291 (1948).

[6] A. D. MacDonald, *Microwave Breakdown in Gases*, Wiley, New York (1966).

[7] F. Paschen, "Ueber die zum Funkenübergang in Luft, Wasserstoff und Kohlensäure bei verschiedenen Drucken erforderliche Potentialdifferenz", *Annalen der Physik*, **273**, 5, 69 (1889).

[8] P. T. Farnsworth, "Television by Electron Image Scanning", *J. Franklin Inst.*, **218**, 4, 411 (1934).

[9] H. A. Lorentz, *The Theory of Electrons*, Second Edition, B. G. Teubner, Leipzig (1916).

[10] Yu. P. Raizer, *Gas Discharge Physics*, Springer, Berlin (1971).

[11] R. Udiljak, D. Anderson, M. Lisak, V. E. Semenov and J. Puech, "Multipactor in low pressure gas", *Phys. Plasmas*, **10**, 10, 4105 (2003).

[12] R. Fante, "Mathematical Analysis of Microwave Breakdown in Flowing Gases", *IEEE Trans. Antennas and Propagation*, **13**, 5, 781 (1965).

[13] M. Gilden, and J. Pergola, "Microwave Breakdown Near a Hot Surface", *IEEE Trans. Microwave Theory and Techniques*, **12**, 1, 26 (1964).

[14] M. Mitchner, and C. H. Kruger, Jr., *Partially Ionized Gases*, John Wiley & Sons Inc., United States (1973).

[15] A. Aleksandrov, V. Bychkov, L. Grachev, I. Esakov, and A. Lomteva, "Air Ionization in a Near-Critical Electric Field", *Technical Physics*, **51**, 3, 330 (2006).

[16] W. Woo, and J. S. DeGroot, "Microwave Absorption and Plasma Heating due to Microwave Breakdown in the Atmosphere", *Phys. Fluids*, **27**, 2, 475 (1984).

[17] W. C. Taylor, W. E. Scharfman and T. Morita, *Voltage Breakdown of Microwave Antennas*, Advances in Microwaves vol 7 (ed L. Young), New York: Academic (1971).

[18] R. L. Fante, J. M. Yos, and J. J. Otazo, *Simple Analytical Models for Calculating Breakdown in Air-Filled Transmission Systems*, Technical Report AFCRL-71-0206, U. S. Air Force Cambridge Research Laboratory (1971).

[19] K. Papadopoulos, G. Milikh, A. Gurevich, A. Drobot, and R. Shanny, "Ionization Rates for Atmospheric and Ionospheric Breakdown", *J. Geophys. Res.*, **98**, A10, 17593 (1993).

[20] Yu. A. Lupan "Refined Theory for an RF Discharge in Air", *Soviet Physics Technical Physics*, **21**, 11, 1367 (1976).

[21] A. W. Ali, *Intense and Short Pulse Electric Field (DC and Microwave) Air Breakdown Parameters*, NRL Memorandum Report 5815, Washington (1986).

[22] W. Scharfman, and T. Morita "Focused Microwave Technique for Measurement of the Ionization Rate and Collision Frequency", *J. Appl. Phys.*, **35**, 7, 2016 (1964).

[23] M. A. Harrison, and R. Geballe, "Simultaneous Measurement of Ionization and Attachment Coefficients", *Physical Review*, **91**, 1, 1 (1953).

[24] E. Kuffel, W. S. Zaengl, and J. Kuffel, *High Voltage Engineering, Fundamentals*, Second Edition, Butterworth-Heinemann, Oxford (2000).

[25] M. J. Druyvesteyn, and F. M. Penning, "The Mechanism of Electrical Discharges in Gases of Low Pressure", *Reviews of Modern Physics*, **12**, 2, 87 (1940).

[26] J. C. Maxwell, *Theory of Heat*, Longmans Green and Co., London (1899).

[27] J. S. Townsend, and H. T. Tizard, "The Motion of Electrons in Gases", *Proc. Roy. Soc. London A*, **88**, 604, 336 (1913).

[28] S. E. El-Khamy, "The Theory of Transient Microwave Heating and Ionization of Low-Pressure Air", *J. Phys. D: Appl. Phys.*, **7**, 4, 581 (1974).

[29] S. B. Cohn, "Rounded Corners in Microwave High-Power Filters and Other Components", *IRE Trans. Microwave Theory Techniques*, **9**, 5, 389 (1961).

[30] U. Jordan, D. S. Dorozhkina, V. Semenov, D. Anderson, M. Lisak, J. Puech, I. Nefedov, and I. Shereshevskii, "Microwave Breakdown in RF Devices Containing Sharp Corners", *IEEE MTT-S International Microwave Symposium Digest*, 1233 (2006).

[31] L. D. Landau, E. M. Lifshitz, and L. P. Pitaevskii, *Electrodynamics of continuous media*, Butterworth Heineman, Oxford, 2nd edition (2008).

[32] Yu. Raizer, "Propagation of a High Pressure Microwave Discharge", *JETP*, **34**, 1, 114 (1972).

[33] V. E. Semenov, "Breakdown Wave in the Self-Consistent Field of an Electromagnetic Wave Beam", *Soviet Journal of Plasma Physics*, **8**, 3, 347 (1982).

[34] D. Anderson, M. Lisak, and T. Lewin, "Self-Consistent Structure of an Ionization Wave Produced by Microwave Breakdown in Atmospheric Air", *Phys. Fluids*, **29**, 2, 446 (1986).

[35] V. B. Gil'denburg, V. L. Gol'tsman, and V. E. Semenov, "A Nonequilibrium High-Frequency Discharge in Quasistatic Fields", *Radiophysics and Quantum Electronics*, **17**, 11, 1312 (1974).

[36] V. B. Gil'denburg, and V. E. Semenov, "Steady State Configurations of Nonequilibrium RF Discharges in Quasistatic Fields", *Soviet Journal of Plasma Physics*, **6**, 2, 244 (1980).

[37] V. E. Semenov, "Multilayer Discharge Structure in the Self-Consistent Field of Two Quasioptical Beams of Electromagnetic Waves", *Soviet Journal of Plasma Physics*, **10**, 3, 328 (1984).

[38] R. G. Forbes, C. J. Edgcombe, and U. Valdrè, "Some Comments on Models for Field Enhancement", *Ultramicroscopy*, **95**, 58 (2003).

[39] J. A. Stratton, *Electromagnetic Theory*, McGraw-Hill, New York (1941).

[40] G. Mie, "Beiträge zur Optik trüber Medien, speziell kolloidaler Metallösungen", *Annalen der Physik*, **25**, 3, 377 (1908).

[41] Y. A. Çengel, *Heat and Mass Transfer, A Practical Approach*, 3rd ed., McGraw-Hill, New York (2007).

[42] A. S. Acampora and P. T. Sproul, "Waveguide Breakdown Effects at High Average Power and Long Pulse Length", *The Bell System Technical Journal*, **51**, 9, 2065 (1972).

[43] W. Beust and W. Ford, "Arcing in CW Transmitters", *Microwave Journal*, **10**, 91 (1961).

[44] M. Nakamura, T. Saito and M. Kuramoto, "Characteristics of High Power Breakdown at 28 GHz", *IEEE Transactions on Microwave Theory and Techniques*, **MTT-26**, 5, 354 (1978).

[45] H. Bruining, *Physics and Applications of Secondary Electron Emission*, Pergamon Press, London (1954).

[46] J. R. M. Vaughan, "A New Formula for Secondary Emission Yield", *IEEE Trans. Electron Devices*, **36**, 9, 1963 (1989).

[47] E. W. B. Gill, and A. von Engel, "Starting Potentials of High-Frequency Gas Discharges at Low Pressure", *Proc. Roy. Soc. London A*, **192**, 1030, 446 (1948).

[48] M. H. Greenblatt, "A Microwave Secondary Electron Multiplier", *Review of Scientific Instruments*, **20**, 9, 646 (1949).

[49] G. Francis, and A. von Engel, "The Growth of the High-Frequency Electrodeless Discharge", *Proc. Roy. Soc. London A*, **246**, 909, 143 (1953).

[50] A. J. Hatch, and H. B. Williams, "The Secondary Electron Resonance Mechanism of Low-Pressure High-Frequency Gas Breakdown", *J. Appl. Phys.*, **25**, 4, 417 (1954).

[51] A. J. Hatch, and H. B. Williams, "Multipacting Modes of High-Frequency Gaseous Breakdown", *Phys. Rev.*, **112**, 3, 681 (1958).

[52] V. E. Semenov, N. A. Zharova, D. Anderson, M. Lisak, and J. Puech, "Simulations of multipactor in circular waveguides", *Phys. Plasmas*, **17**, 2, 123503 (2010).

[53] A. G. Sazontov, V. A. Sazontov, and N. K. Vdovicheva, "Multipactor breakdown prediction in a rectangular waveguide", *Contrib. Plasma Phys.*, **48**, 4, 331 (2008).

[54] V. E. Semenov, E. I. Rakova, D. Anderson, M. Lisak, and J. Puech, "Multipactor in rectangular waveguides", *Phys. Plasmas*, **14**, 3, 033501 (2007).

[55] R. Udiljak, D. Anderson, M. Lisak, V. E. Semenov, and J. Puech, "Multipactor in a coaxial transmission line. I. Analytical study", *Phys. Plasmas*, **14**, 033508 (2007).

[56] A. M. Perez, C. Tienda, C. Vicente, A. Goves, G. Torregrosa, B. Gimeno, R. Barcot, V. E. Boria, and D. Raboso, "Multipactor analysis in coaxial waveguides for satellite applications using frequency-domain methods", *IEEE MTT-S Int. Microw. Symp. Dig.*, 1045-1048 (2006).

[57] V. E. Semenov, N. Zharova, R. Udiljak, D. Anderson, M. Lisak, and J. Puech, "Multipactor in a coaxial transmission line. II. Particle-in-cell simulations", *Phys. Plasmas*, **14**, 3, 033509 (2007).

[58] A. M. Perez, C. Tienda, C. Vicente, S. Anzam, J. Gil, B. Gimeno, V. E. Boria, and D. Raboso, "Prediction of multipactor breakdown thresholds in coaxial transmission lines for travelling, standing, and mixed waves", *IEEE Trans. Plasma Sci.*, **37**, 10, 2031 (2009).

[59] V. E. Semenov, E. Rakova, N. Zharova, D. Anderson, M. Lisak, and J. Puech, "Simulations of the multipactor effects in hollow waveguides with wedge-shaped cross section", *IEEE Trans. Plasma Sci.*, **36**, 2, 488 (2008).

[60] J. Hueso, C. Vicente, B. Gimeno, V. E. Boria, S. Marini, and M. Taroncher, "Multipactor effect analysis and design rules for wedge-shaped hollow waveguides", *IEEE Trans. Electron Dev.*, **57**, 12, 3508 (2010).

[61] V. E. Semenov, E. Rakova, R. Udiljak, D. Anderson, M. Lisak, and J. Puech, "Conformal mapping analysis of multipactor breakdown in waveguide irises", *Phys. Plasmas*, **15**, 3, 033501 (2008).

[62] V. E. Semenov, A. Kryazhev, D. Anderson, and M. Lisak, "Multipactor Suppression in Amplitude Modulated Radio Frequency Fields", *Phys. Plasmas*, **8**, 11, 5034 (2001).

[63] S. Anza, C. Vicente, B. Gimeno, V. E. Boria, and J. Armendariz, "Long-Term Multipactor Discharge in Multicarrier Systems", *Phys. Plasmas*, **14**, 8, 082112 (2007).

[64] V. Semenov, M. Buyanova, D. Anderson, M. Lisak, R. Udiljak, and J. Puech, "Multipactor in Microwave Transmission Systems Using Quadrature Phase-Shift Keying", *IEEE Trans. Plasma Sci.*, **38**, 4, 915 (2010).

[65] N. K. Vdovicheva, A. G. Sazontov, and V. E. Semenov, "Statistical theory of two-sided multipactor", *Radiophys. Quantum Electron.*, **47**, 8, 580 (2004).

[66] N. K. Vdovicheva, A. G. Sazontov, V. A. Sazontov, and V. E. Semenov, "Influence of the angular anisotropy of secondary emission on the characteristics of two-sided multipactor", *Radiophys. Quantum Electron.*, **49**, 5, 368 (2006).

[67] A. Sazontov, M. Buyanova, V. Semenov, E. Rakova, N. Vdovicheva, D. Anderson, M. Lisak, J. Puech, and L. Lapierre, "Effect of emission velocity spread of secondary electrons in two-sided multipactor", *Phys. Plasmas*, **12**, 053102 (2005).

[68] S. Anza, C. Vicente, J. Gil, V. E. Boria, B. Gimeno, and D. Raboso, "Nonstationary statistical theory for multipactor", *Phys. Plasmas*, **17**, 062110 (2010).

[69] A. G. Sazontov, V. A. Sazontov, and N. K. Vdovicheva, "Multipactor Breakdown Prediction in a Rectangular Waveguide: Statistical Theory and Simulation Results", *Contrib. Plasma Phys.*, **48**, 4, 331 (2008).

[70] A. Sazontov, V. Semenov, M. Buyanova, N. Vdovicheva, D. Anderson, M. Lisak, J. Puech, and L. Lapierre, "Multipactor discharge on a dielectric surface: Statistical theory and simulation results", *Phys. Plasmas*, **12**, 093501 (2005).

[71] S. Anza, M. Mattes, C. Vicente, D. Raboso, V. E. Boria, and B. Gimeno, "Multipactor theory for multicarrier signals", *Phys. Plasmas*, **18**, 032105 (2011).

[72] V. A. Stanskii, D. A. Ganichev, and S. A. Fridrikhov, "Calculation of the effective coefficient of secondary electron emission from walls localizing a microwave discharge", *Sov. Phys. Tech. Phys.*, **18**, 8, 1103 (2007).

[73] G. S. Luk'yanchikov, "Multiphase, uniform, secondary-emission microwave discharge at a solid surface", *Sov. Phys. Tech. Phys.*, **19**, 9, 1196 (1975).

[74] L. V. Grishin, and G. S. Luk'yanchikov, "Multipactor discharge with an electron velocity distribution", *Sov. Phys. Tech. Phys.*, **21**, 3, 307 (1976).

[75] A. A. Dorofeyuk, I. A. Kossyi, G. S. Luk'yanchikov, and M. M. Savchenko, "Electron discharge in the interaction of microwave radiation with a metal surface", *Sov. Phys. Tech. Phys.*, **21**, 1, 76 (1976).

[76] A. Kryazhev, M. Buyanova, V. Semenov, D. Anderson, M. Lisak, J. Puech, L. Lapierre, and J. Sombrin, "Hybrid resonant modes of two-sided multipactor and transition to the polyphase regime", *Phys. Plasmas*, **9**, 11, 4736 (2002).

[77] I. A. Kossyi, G. S. Luk'yanchikov, V. E. Semenov, E. I. Rakova, D. Anderson, M. Lisak, and J. Puech, "Experimental Study of the Single-Surface Poly-Phase Multipactor on a Metal Plate", Mulcopim, September 21-23, Valencia, Spain (2011).

[78] J. F. Johansson, and J. Rasch, "Non-Resonant Probabilistic Multipactor Calculations", Mulcopim, September 21-23, Valencia, Spain (2011).

[79] A. V. Gaponov, and M. A. Miller, "Potential Wells for Charged Particles in a High-Frequency Electromagnetic Field", *JETP*, **7**, 168 (1958).

[80] F. F. Chen, *Introduction to Plasma Physics*, Plenum Press, New York (1974).

[81] P. M. Bellan, *Fundamentals of Plasma Physics*, Cambridge University Press (2006).

[82] *Space Engineering, Multipactor Design, and Test*, ECSS-E-20-01-01A, May 5 (2003).